

Fully Asynchronous Distributed Optimization with Linear Convergence in Directed Networks

Jiaqi Zhang, Keyou You

Abstract—We consider the distributed optimization problem, the goal of which is to minimize the sum of local objective functions over a directed network. Though it has been widely studied recently, most of the existing algorithms are designed for synchronized or randomly activated implementation, which may create deadlocks in practice. In sharp contrast, we propose a *fully asynchronous push-pull gradient algorithm (APPG)* where each node updates without waiting for any other node by using (possibly stale) information from neighbors. Thus, it is both deadlock-free and robust to any bounded communication delay. Moreover, we construct two novel augmented networks to theoretically evaluate its performance from the worst-case point of view and show that if local functions have Lipschitz-continuous gradients and their sum satisfies the Polyak-Łojasiewicz condition (convexity is not required), each node of APPG converges to the same optimal solution at a linear rate of $\mathcal{O}(\lambda^k)$, where $\lambda \in (0, 1)$ and the virtual counter k increases by one no matter which node updates. This largely elucidates its linear speedup efficiency and shows its advantage over the synchronous version. Finally, the performance of APPG is numerically validated via a logistic regression problem on the *Coverttype* dataset.

Index Terms—Fully asynchronous, distributed optimization, linear convergence, Polyak-Łojasiewicz condition

I. INTRODUCTION

As data get larger and more spatially distributed, the distributed optimization over a network of computing nodes (aka. agents or workers) has found numerous applications in multi-agent problems [1]–[3] and machine learning [4]–[6]. It aims to minimize the sum of local objective functions, i.e.,

$$\underset{\mathbf{x} \in \mathbb{R}^m}{\text{minimize}} \quad f(\mathbf{x}) := \sum_{i=1}^n f_i(\mathbf{x}) \quad (1)$$

where n is the number of nodes and the local objective function f_i is only known by node i . Nodes are expected to solve (1) by only communicating with neighbors that are defined by the network, see Fig. 1. In the empirical risk minimization problem [6], [7], f_i often takes the form $f_i(\mathbf{x}) := \sum_{\xi \in \mathcal{D}_i} F_i(\mathbf{x}; \xi)$ where \mathcal{D}_i is a local dataset of node i , \mathbf{x} is the model parameter to be optimized, and $F_i(\mathbf{x}; \xi)$ is the loss of a single sample ξ .

For large-scale optimization problems, it is crucial to design an easily implementable algorithm that is robust to heterogeneous nodes and communication delays. Many existing works focus on synchronous algorithms where all nodes essentially start to compute each iteration simultaneously (c.f. Fig. 2(a)) by using a global synchronization scheme that is often not amenable to the distributed setting.

J. Zhang and K. You are with the Department of Automation, and BNRist, Tsinghua University, Beijing 100084, China. E-mail: zjq16@mails.tsinghua.edu.cn, youky@tsinghua.edu.cn.

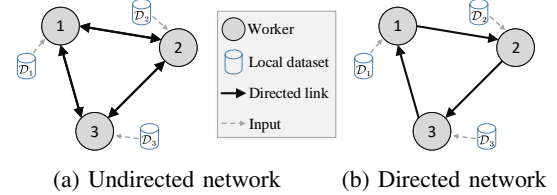


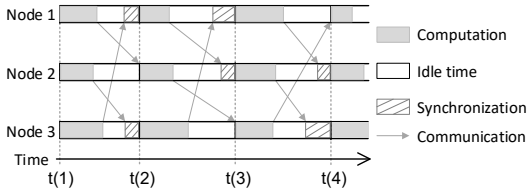
Fig. 1: Undirected and directed peer-to-peer networks.

Asynchronous updates are demonstrated to perform better than synchronous counterparts [4], [8]–[14]. A popular one is gossip-based [4], [9]–[12] where a pair of neighbors is randomly selected to concurrently update via information exchange, see Fig. 2(b). However, this (a) may create deadlocks in practice [4], [15], especially for networks with many cycles, (b) is vulnerable to communication delays, and (c) cannot work on directed networks.

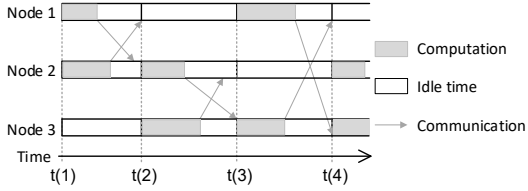
To address these issues simultaneously, this work considers the *fully asynchronous* setting (c.f. Fig 2(c), [13], [16], [17]) over *directed* networks and proposes an asynchronous push-pull gradient (APPG) algorithm to distributedly solve (1). In APPG, a node starts to update without waiting for other nodes by only using locally accessed (possibly stale) information. It does not need any network synchronization, and can tolerate uneven update frequencies and communication delays among nodes.

To theoretically evaluate its performance, we develop an augmented network approach and use the machinery of linear matrix inequalities (LMIs) to capture some key quantities via a novel λ -sequence. If all local functions f_i have Lipschitz continuous gradients and the global objective function f satisfies the Polyak-Łojasiewicz (PL) condition (no convexity requirement), we prove from the worst-case point of view that APPG converges linearly to an optimal solution at a rate $\mathcal{O}(\lambda^k)$ where $\lambda \in (0, 1)$ depends on the asynchrony level and delay bounds, and the virtual counter k increases by one no matter which node updates. Note that the convergence guarantee for gossip-based algorithms is generally given in the stochastic sense.

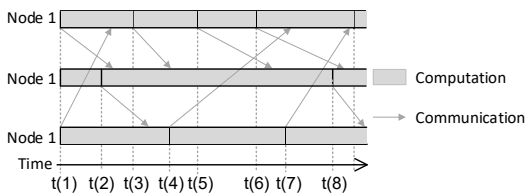
Then, we implement APPG on a multi-core server with the Message Passing Interface (MPI) to solve a multi-class logistic regression problem over the *Coverttype* dataset. The result confirms that its empirical convergence rate in running time is faster than its synchronous counterpart, and achieves linear speedup efficiency with respect to the node number. Its robustness to slow computing nodes is also validated, which is essential in heterogeneous large-scale networks.



(a) A synchronous algorithm over Fig. 1(b). All nodes start new updates simultaneously.



(b) A gossip-based algorithm over Fig. 1(a). A pair of neighboring nodes are selected to concurrently update via information exchange.



(c) A fully asynchronous algorithm over Fig. 1(b). Every node proceeds without waiting for others.

Fig. 2: Synchronous, gossip-based, and fully asynchronous algorithms over the network in Fig. 1.

The rest of the paper is organized as follows. Section II briefly reviews some related works. Section III formulates the problem and proposes APPG. We provide the theoretical results for APPG in Section IV. To prove them, we first develop a time-varying augmented network approach in Section V, and then establish the LMIs in Section VI. In Section VII, we conduct numerical experiments on APPG. Some concluding remarks are drawn in Section VIII.

II. RELATED WORK

The past decade has witnessed an increasing attention on distributed optimization, especially for the design of synchronous algorithms, e.g., DGD [1], EXTRA [18], DIGing [19], [20], MSDA [21], NIDS [22], ABC [23], DSGT [6] and [24]–[28]. The row-stochastic matrix [29], epigraph reformulation [30] and the push-sum method [5], [31], [32] have also been proposed to solve the network unbalancedness issue. For example, Push-DIGing [19] combines the push-sum method and gradient tracking [12], [19], [20] to achieve linear convergence for strongly convex and Lipschitz smooth functions. However, it involves nonlinear operators per update, which is solved in the push-pull/AB algorithm [33]–[35].

The recent interest has been shift to asynchronous algorithms. The gossip-based AsynDGM [12] assumes that each pair of neighbors is activated to update with a fixed probability, and has been extended in [4] where the activated nodes admit a doubly-stochastic mixing matrix. Ref. [9] considers that each node is activated by a Poisson process. Though they

can be applied to directed networks, the coordination between neighbors is indispensable.

Inspired by the seminal works [36], [37], the fully asynchronous setting has emerged as a more scalable and easier implementable alternative. An initial attempt is made in [17] to extend the synchronous gradient-push algorithm [31] to this setting. However, they cannot achieve exact convergence to an optimal solution if nodes have different update frequencies. To address it, Ref. [13] proposes a novel adaptive mechanism to dynamically adjust stepsize, which is also adopted in [38] to analyze stochastic algorithms. Nonetheless, the algorithms in [13], [38] only have sublinear convergence rates even if the objective function is strongly convex and Lipschitz smooth. Asy-SONATA [16] exploits the perturbed push-sum method with gradient tracking ([12], [19], [20]) in the fully asynchronous setting, and converges (a) linearly for strongly convex and Lipschitz smooth functions, and (b) sublinearly for non-convex problems. The striking differences between [16] and our work include: (a) APPG further converges linearly even under the PL condition, which holds for some important non-convex problems, e.g., the policy optimization for LQR [39]. (b) APPG uses uncoordinated constant stepsizes while Asy-SONATA can only use uncoordinated diminishing stepsizes, which however leads to a sublinear convergence rate. (c) APPG seems easier to understand and implement.

Notation: Throughout this paper, we use the following notation and definitions:

- a , \mathbf{a} , A , and \mathcal{A} generally denote respectively a scalar, column vector, matrix, and set. $(\cdot)^\top$ denotes the transpose.
- \mathbb{R}^n and \mathbb{N} denote the set of n -dimensional real numbers and natural numbers, respectively.
- $\|\cdot\|_2$ denotes the l_2 -norm of a vector or matrix. $\|\cdot\|_F$ denotes the matrix Frobenius norm. $\mathcal{O}(\cdot)$ denotes the big-O notation.
- $\mathbf{1}_n$ and $\mathbf{0}_n$ denote respectively the n -dimensional vector with all ones and all zeros, where the subscript is omitted if the dimension is clear from the context.
- $\nabla f(x)$ denotes the gradient of a function f at x .
- \mathbf{a} is called a stochastic vector if it is nonnegative and $\mathbf{a}^\top \mathbf{1} = 1$. A is called a row-stochastic matrix if A is nonnegative and $A\mathbf{1} = \mathbf{1}$. A is column-stochastic if A^\top is row-stochastic. A is doubly-stochastic if A is both row- and column-stochastic.
- $[A]_{ij}$ denotes the element in row i and column j of A .
- $|\mathcal{A}|$ denotes the cardinality of \mathcal{A} .
- $\lfloor x \rfloor$ denotes the largest integer less than or equal to x .
- $[\mathbf{a}_1, \mathbf{a}_2, \dots, \mathbf{a}_n]$ and $[\mathbf{a}_1; \mathbf{a}_2; \dots; \mathbf{a}_n]$ denote the horizontal stack and vertical stack of $\mathbf{a}_1, \mathbf{a}_2, \dots, \mathbf{a}_n$, respectively.
- $\text{Proj}_{\mathcal{X}}(\mathbf{x})$ denotes the projection of \mathbf{x} onto the set \mathcal{X} .

III. THE APPG

A. Problem formulation

We aim to solve (1) over a directed network. A directed network (digraph) is denoted by $\mathcal{G} = (\mathcal{V}, \mathcal{E})$, where $\mathcal{V} = \{1, 2, \dots, n\}$ is the set of nodes and $\mathcal{E} \subseteq \mathcal{V} \times \mathcal{V}$ is the set of edges. The directed edge $(i, j) \in \mathcal{E}$ if node i can directly send information to node j . Let $\mathcal{N}_{\text{in}}^i = \{j | (j, i) \in \mathcal{E}\} \cup \{i\}$ denote the set of in-neighbors of node i and $\mathcal{N}_{\text{out}}^i = \{j | (i, j) \in \mathcal{E}\} \cup \{i\}$ denote the set of out-neighbors of i . A path from node

i to node j is a sequence of consecutively directed edges from node i to node j . Then, \mathcal{G} is *strongly connected* if there exists a directed path between any pair of nodes. For a strongly connected graph \mathcal{G} , the distance between two nodes is the minimum number of edges to connect them via a directed path, and the largest distance d_g is also called its diameter.

For a distributed algorithm over \mathcal{G} , each node i has a local state vector \mathbf{x}_i and iteratively update it via directed communications with neighbors, the objective of which is to ensure all local states $\mathbf{x}_i, i \in \mathcal{V}$ converge to an optimal solution of (1). In this work, we make the following assumptions.

Assumption 1:

- (a) The digraph \mathcal{G} is strongly connected.
- (b) All local functions f_i are β -Lipschitz smooth, i.e., there exists a $\beta > 0$ such that

$$\|\nabla f_i(\mathbf{x}) - \nabla f_i(\mathbf{y})\|_2 \leq \beta \|\mathbf{x} - \mathbf{y}\|_2, \quad \forall i \in \mathcal{V}, \mathbf{x}, \mathbf{y} \in \mathbb{R}^m.$$

- (c) The global objective function f has at least one minimizer and satisfies the Polyak-Łojasiewicz condition [40] with parameter $\alpha > 0$, i.e., $\mathcal{X}^* = \operatorname{argmin}_{\mathbf{x} \in \mathbb{R}^m} f(\mathbf{x}) \neq \emptyset$, and

$$2\alpha(f(\mathbf{x}) - f^*) \leq \|\nabla f(\mathbf{x})\|_2^2, \quad \forall \mathbf{x} \in \mathbb{R}^m,$$

where $f^* = \min_{\mathbf{x} \in \mathbb{R}^m} f(\mathbf{x})$.

Assumptions 1(a)-(b) are standard in the distributed smooth optimization over directed networks [19], [33]. The PL condition in Assumption 1(c) is satisfied in some important *non-convex* problems such as the policy optimization for LQR [39]. It is strictly weaker than the strongly convex condition that is commonly used to derive the linear convergence of gradient-based methods [16], [19]. Particularly, the strong convexity implies the uniqueness of the minimizer, which is clearly not the case for the PL condition.

B. The APPG

The details of APPG are given in Algorithm 1, where we do not introduce any iteration index to emphasize the fact of fully asynchronous implementation.

From the view of a single node, we illustrate the easy implementation of APPG. Our novel idea lies in the use of local buffers in each node. Particularly, a node just keeps receiving messages from its in-neighbors and storing them to its local buffers until it is activated to compute a new update. Clearly, each buffer may contain zero, one or multiple receptions from the same in-neighbor, which is unavoidable in the fully asynchronous setting. Another striking feature of APPG is that the node computes a new update by using all messages in the buffers (c.f. (2)), instead of only using the latest reception. This enables APPG to be robust to bounded communication delays, out of sequence issues and there is no need to use any iteration index, which is required by Asy-SONATA [16]. Interestingly, the local buffers can also be waived since the average and summation operators in (2) can be recursively computed. Next, the node broadcasts the updated vectors to its out-neighbors, after which empties its buffers. Such a process is repeated until a local stopping criterion (e.g., $\|\mathbf{y}_i\|_2 < \epsilon$) is satisfied.

Algorithm 1 The APPG — from the view of node i

- **Initialization:** Each node i selects local stepsize γ_i , initializes \mathbf{x}_i as an arbitrary real vector in \mathbb{R}^m , computes $\mathbf{g}_i = \mathbf{y}_i = \nabla f_i(\mathbf{x}_i)$, and creates local buffers \mathcal{X}_i and \mathcal{Y}_i . Then it broadcasts $\tilde{\mathbf{x}}_i := \mathbf{x}_i$ and $\tilde{\mathbf{y}}_i := \mathbf{y}_i/|\mathcal{N}_{\text{out}}^i|$ to its out-neighbors.

- **Repeat**

- 1: Keep receiving $\tilde{\mathbf{x}}_j$ and $\tilde{\mathbf{y}}_j$ from in-neighbors of node i and copy to \mathcal{X}_i and \mathcal{Y}_i respectively¹, until node i is activated to update.
- 2: Update \mathbf{x}_i and \mathbf{y}_i as

$$\begin{aligned} \mathbf{x}_i &\leftarrow \mathbf{avg}(\mathcal{X}_i) \\ \mathbf{g}_i^- &\leftarrow \mathbf{g}_i, \quad \mathbf{g}_i \leftarrow \nabla f_i(\mathbf{x}_i) \\ \mathbf{y}_i &\leftarrow \mathbf{sum}(\mathcal{Y}_i) + \mathbf{g}_i - \mathbf{g}_i^- \\ \tilde{\mathbf{x}}_i &\leftarrow \mathbf{x}_i - \gamma_i \mathbf{y}_i \end{aligned} \quad (2)$$

where $\mathbf{avg}(\mathcal{X}_i)$ returns the average² of vectors in \mathcal{X}_i , $\mathbf{sum}(\mathcal{Y}_i)$ takes the sum of vectors in \mathcal{Y}_i . $\tilde{\mathbf{x}}_i$, \mathbf{g}_i^- and \mathbf{g}_i are three auxiliary vectors.

- 3: Broadcast $\tilde{\mathbf{x}}_i$ and $\tilde{\mathbf{y}}_i := \mathbf{y}_i/|\mathcal{N}_{\text{out}}^i|$ to all out-neighbors of i , after which *empty* both \mathcal{X}_i and \mathcal{Y}_i .

- **Until** a stopping criterion is satisfied. e.g., node i stops if $\|\mathbf{y}_i\|_2 < \epsilon$ for some predefined $\epsilon > 0$.

- **Return** \mathbf{x}_i .
-

¹The set of in-neighbors includes i itself, i.e., $\tilde{\mathbf{x}}_i$ and $\tilde{\mathbf{y}}_i$ are copied to \mathcal{X}_i and \mathcal{Y}_i .

²The average can be weighted, e.g., one may assign higher weights to more recent messages to potentially improve the convergence rate in practice.

Different from synchronous or gossip-based algorithms, APPG does not require any global clock or coordination among nodes, and each node does not wait for others for new updates. For example, a node can simply start to compute a new update once it completes the current one. Thus, there is no deadlock problem in APPG. Moreover, the local stepsize γ_i can be different among nodes.

C. The idea of APPG

This subsection aims to intuitively explain the linear convergence of the APPG. To this end, we first show how APPG works if nodes are forced to update synchronously. In this case, we can use a global iteration index k to record the update progress.

Let $X(k)$, $Y(k)$ and $\nabla \mathbf{f}(X(k))$ be the stacked local states and gradients at the k -th iteration, i.e.,

$$X(k) = [\mathbf{x}_1(k), \mathbf{x}_2(k), \dots, \mathbf{x}_n(k)]^T \in \mathbb{R}^{n \times m}$$

$$Y(k) = [\mathbf{y}_1(k), \mathbf{y}_2(k), \dots, \mathbf{y}_n(k)]^T \in \mathbb{R}^{n \times m}$$

$$\nabla \mathbf{f}(X(k)) = [\nabla f_1(\mathbf{x}_1(k)), \dots, \nabla f_n(\mathbf{x}_n(k))]^T \in \mathbb{R}^{n \times m}$$

and $\Gamma = \operatorname{diag}(\gamma_1, \dots, \gamma_n)$. Then, we obtain that

$$X(k+1) = A(X(k) - \Gamma Y(k)) \quad (3a)$$

$$Y(k+1) = B Y(k) + \nabla \mathbf{f}(X(k+1)) - \nabla \mathbf{f}(X(k)) \quad (3b)$$

where the row-stochastic matrix A and column-stochastic matrix B result from $\mathbf{avg}(\cdot)$ and $\mathbf{sum}(\cdot)$ in (2), respectively.

Clearly, (3) reduces to the algorithm in [33]–[35], which has been proved to converge linearly for strongly convex and Lipschitz smooth functions.

The key to the linear convergence of (3) is the introduction of \mathbf{y}_i to distributedly track the gradient of f . Then, we left multiply (3b) with $\mathbf{1}^\top$, use the column-stochasticity of B and notice $Y(0) = \nabla f(X(0))$. This implies that

$$\mathbf{1}^\top Y(k) = \mathbf{1}^\top \nabla f(X(k)). \quad (4)$$

Now suppose that $X(k)$ and $Y(k)$ have already converged to X^∞ and Y^∞ , respectively. It follows from (3b) that $Y^\infty = BY^\infty$. Jointly with (4), we obtain that

$$\mathbf{y}_i^\infty = \pi_i^B (\mathbf{1}^\top \nabla f(X^\infty))^\top$$

where π^B is the Perron vector of B , i.e. $B\pi^B = \pi^B$. Moreover, the row-stochasticity of A implies that $X^\infty = \mathbf{1}(\mathbf{x}^\infty)^\top$ and

$$(\mathbf{1}^\top \nabla f(X^\infty))^\top = (\mathbf{1}^\top \nabla f(\mathbf{1}(\mathbf{x}^\infty)^\top))^\top = \nabla f(\mathbf{x}^\infty).$$

That is, $\mathbf{y}_i^\infty = \pi_i^B \nabla f(\mathbf{x}^\infty)$. Substituting X^∞ and Y^∞ into (3a) implies

$$X(k+1) = A(X^\infty - \Gamma \pi^B \nabla f(\mathbf{x}^\infty)^\top).$$

Let π^A be Perron vector of A^\top . We left multiply (3a) with $(\pi^A)^\top$ and notice that $X^\infty = \mathbf{1}(\mathbf{x}^\infty)^\top$. Then,

$$\mathbf{x}(k+1) = \mathbf{x}^\infty - (\pi^A)^\top \Gamma \pi^B \nabla f(\mathbf{x}^\infty) = \mathbf{x}^\infty - \rho \nabla f(\mathbf{x}^\infty) \quad (5)$$

where $\rho = (\pi^A)^\top \Gamma \pi^B$. Clearly, (5) is a gradient descent update, which converges linearly under Assumption 1. It also shows that the limiting point \mathbf{x}^∞ must be an optimal point \mathbf{x}^* and \mathbf{y}_i converges to $\mathbf{y}_i^\infty = \pi_i^B \nabla f(\mathbf{x}^\infty) = \pi_i^B \nabla f(\mathbf{x}^*) = 0$. Moreover, the smaller the \mathbf{y}_i , the closer \mathbf{x}_i to an optimal solution. Therefore, \mathbf{y}_i can serve as a stopping criterion in Algorithm 1.

In the fully asynchronous setting, \mathbf{y}_i plays a similar role. However, a theoretical understanding of APPG is much more complicated. The information delays make the key relation (4) invalid and the uncoordinated updates degrade the tracking performance of \mathbf{y}_i . In essence, APPG is a multi-timescale decision-making problem. To resolve it, we develop an augmented network approach to prove its linear convergence by associating each node with some virtual nodes, under which the asynchronous updates and communications of nodes are transformed into synchronous operations over the augmented network. Moreover, the key technique in [33]–[35] cannot be applied since the transformed system is time-varying and lacks their important properties (e.g. the irreducibility of the weighting matrix). To this end, we further design an absolute probability sequence and a λ -sequence for the proof.

IV. LINEAR CONVERGENCE OF APPG

Two assumptions on the asynchronism and communication delays are needed for the convergence of APPG.

Assumption 2 (Bounded activation time interval): Let t_i and t_i^+ be any two consecutive activation time of node i . There exist two positive constants $\underline{\tau}$ and $\bar{\tau}$ such that $0 < \underline{\tau} \leq |t_i^+ - t_i| \leq \bar{\tau} < \infty$ for all $i \in \mathcal{V}$.

Assumption 2 is easily satisfied and desirable in practice. In fact, both the lower and upper bounds exist naturally since computing update consumes time and can be finished in finite time. If violated, e.g., some node is broken, then the information from this node can no longer be accessed, and hence it is impossible to find an optimal solution of (1).

Assumption 3 (Bounded transmission delays): For any $(i, j) \in \mathcal{E}$, the transmission delay from node i to node j is bounded by a constant $\tau > 0$.

Note that transmission delays can be time-varying, and the parameters $\underline{\tau}$, $\bar{\tau}$ and τ are not needed for implementing APPG.

Let $\mathcal{T} = \{t(k)\}_{k \geq 1}$ be an increasing sequence of updating time of all nodes, i.e., $t \in \mathcal{T}$ if some node starts to update at time t . Denote the state of node i just before time $t(k)$ by $\mathbf{x}_i(k)$ and $\mathbf{y}_i(k)$. Our main theoretical result is given below.

Theorem 1: Suppose that Assumptions 1-3 hold. Let $\bar{\gamma} = \max_i \gamma_i$ and $\underline{\gamma} = \min_i \gamma_i$. If $\bar{\gamma}$ is sufficiently small and $\lambda \in \left(\max\left\{1 - \frac{1-\theta}{2\bar{t}}, 1 - \frac{\gamma\alpha\theta n}{8b}\right\}, 1\right)$, then there exists an optimal solution $\mathbf{x}^* \in \mathcal{X}^*$ such that

$$\|\mathbf{x}_i(k) - \mathbf{x}^*\|_2 = \mathcal{O}(\lambda^k), \quad \|\mathbf{y}_i(k)\|_2 = \mathcal{O}(\lambda^k), \quad \forall i \in \mathcal{V} \quad (6)$$

where α is given in Assumption 1, $b = n(\bar{\tau} + \tau)/\underline{\tau}$. The positive constants $\theta \in (0, 1)$ and \bar{t} are given in Lemmas 2 and 3 of Section V-B, respectively.

Theorem 1 shows that the local decision vector of each node in APPG converges to the same optimal solution at a linear rate. To obtain a deterministic convergence rate, we have to adopt the *worst-case* point of view under the setting that (a) The underlying network is heavily unbalanced, i.e., the differences between the numbers of in-neighbors and out-neighbors of a node is large. (b) Some nodes compute much faster than the others (match the lower and upper bounds of Assumption 2, respectively). (c) Communication delays are based on the upper bound in Assumption 3. Thus, the theoretical rate is expected to be very conservative though the practical performance is empirically much better.

Roughly speaking, b measures the degree of the asynchronicity and delays in the network. Under Assumptions 2 and 3, information sent from a node can be received and used by another node in b steps. θ and \bar{t} reflect the rate of achieving consensus.

The striking feature is that the virtual counter k in (6) increases by one no matter which node updates, and hence more nodes generally lead to faster increase of k . To some extent, this suggests a linear speedup efficiency [4] of APPG, which is confirmed via experiments in Section VII.

V. THE TIME-VARYING AUGMENTED SYSTEM

This section develops our time-varying augmented network approach for the convergence analysis. We first provide a lemma on Assumptions 2 and 3.

Lemma 1: The following statements hold.

- (a) Under Assumption 2, let $b_1 = (n-1)\lfloor \bar{\tau}/\underline{\tau} \rfloor + 1$. Each node is activated at least once within the time interval $(t(k), t(k+b_1)]$.
- (b) Under Assumptions 2 and 3, let $b_2 = n\lfloor \tau/\underline{\tau} \rfloor$ and $b = b_1 + b_2$. The information sent from node i at time $t(k)$

can be received by node j before time $t(k+b_2)$ and used to compute an update before time $t(k+b)$ for any k and $(i, j) \in \mathcal{E}$.

Proof: (a) Suppose that node i is not activated during the time interval $(t(p), t(q)]$, $p, q \in \mathbb{N}$ but is activated at $t(q+1)$. It follows from Assumption 2 that $t(q) - t(p) \leq \bar{\tau}$. Moreover, any other node can be activated at most $\lfloor (t(q) - t(p))/\underline{\tau} \rfloor \leq \lceil \bar{\tau}/\underline{\tau} \rceil$ times during the time interval $(t(p), t(q)]$, which implies $q - p \leq (n-1)\lceil \bar{\tau}/\underline{\tau} \rceil$. Hence, the first part of the result follows.

(b) Suppose that node i sends information at time $t(p)$, $p \in \mathbb{N}$ and node j receives it in the time interval $(t(q), t(q+1)]$, $q \in \mathbb{N}$. It follows from Assumption 3 that $t(q) - t(p) \leq \tau$. Moreover, Assumption 2 implies that any node can be activated at most $\lfloor \tau/\underline{\tau} \rfloor$ times during the time interval $[t(p), t(q)]$, i.e., $q - p + 1 \leq n\lfloor \tau/\underline{\tau} \rfloor$, and hence $q + 1 \leq p + n\lfloor \tau/\underline{\tau} \rfloor$. The result follows by letting $p = k$. Jointly with Lemma 1(a), the rest of proof follows immediately. ■

A. Construction of the augmented digraph

Let $\mathcal{T}_i \subseteq \mathcal{T}$ be the sequence of activation time of node i , i.e., $t \in \mathcal{T}_i$ if node i computes an update at time t . Then, it is clear that

$$\begin{aligned} & [\mathbf{x}_i(k+1), \mathbf{y}_i(k+1), \mathbf{g}_i(k+1), \mathbf{g}_i^-(k+1)] \\ &= [\mathbf{x}_i(k), \mathbf{y}_i(k), \mathbf{g}_i(k), \mathbf{g}_i^-(k)], \quad \forall t(k) \notin \mathcal{T}_i. \end{aligned}$$

To handle bounded time-varying transmission delays and asynchronicity, we design an augmented system. Firstly, we associate each node i with two types of virtual nodes, and each type has b virtual nodes, where b is given in Lemma 1(b). We denote the above two types of virtual nodes by $\{v_{x,i}^{(1)}, \dots, v_{x,i}^{(b)}\}$ and $\{v_{y,i}^{(1)}, \dots, v_{y,i}^{(b)}\}$, respectively. We call the first type virtual nodes x -type nodes, which is to deal with the staleness of the state $\tilde{\mathbf{x}}_i$, $i \in \mathcal{V}$. The second type with subscript y is called y -type nodes, which is to handle the staleness of $\tilde{\mathbf{y}}_i$, $i \in \mathcal{V}$. Then, we construct an augmented digraph $\tilde{\mathcal{G}}(k) = (\tilde{\mathcal{V}}, \tilde{\mathcal{E}}(k))$ to represent the communication topology of all these nodes at time $t(k)$, where $\tilde{\mathcal{V}}$ contains $n(2b+1)$ nodes, including n nodes of \mathcal{G} and $2nb$ virtual nodes.

The edge set $\tilde{\mathcal{E}}(k)$ is described as follows. We first note that there is no edge between any x -type node and any y -type node. For the x -type virtual nodes, the edges $(i, v_{x,i}^{(1)}), (v_{x,i}^{(1)}, v_{x,i}^{(2)}), \dots, (v_{x,i}^{(b-1)}, v_{x,i}^{(b)})$ and $(v_{x,i}^{(b-1)}, v_{x,i}^{(b)})$ always include for all $k \in \mathbb{N}$ and $i \in \mathcal{V}$ (c.f. Fig. 3). If $(i, j) \in \mathcal{E}$ in \mathcal{G} and node j receives $\tilde{\mathbf{x}}_i$ at time $t(k)$, then some of the edges $(v_{x,i}^{(1)}, j), (v_{x,i}^{(2)}, j), \dots, (v_{x,i}^{(b)}, j)$ and (i, j) are included in $\tilde{\mathcal{E}}(k)$ (c.f. Fig. 4(a)), depending on the transmission delay of the received message. If node j receives $\tilde{\mathbf{x}}_i(t-u)$ and $\tilde{\mathbf{x}}_i(t-v)$ at time $t(k)$ for some $u, v > 1$, then $(v_{x,i}^{(u-1)}, j), (v_{x,i}^{(v-1)}, j) \in \tilde{\mathcal{E}}(k)$. If $u = 1$, which means that there is no communication delay, then $(i, j) \in \tilde{\mathcal{E}}(k)$. Fig. 4(a) illustrates such an augmented graph¹.

¹The idea of adding virtual nodes to address asynchronicity or delays was firstly adopted in [41] to study consensus problems and in [13], [16], [17] for distributed optimization. Nevertheless, Refs. [13], [17], [41] use only x -type virtual nodes, and hence involve division operators. We further introduce y -type nodes to accommodate linear update rules. Ref. [16] associates virtual nodes to original edges rather than original nodes.

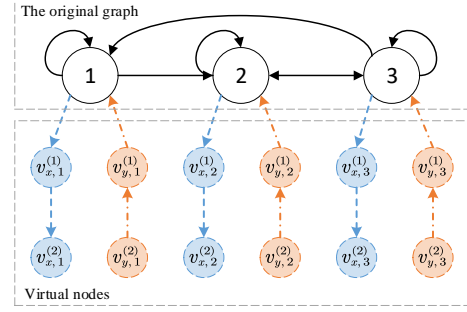


Fig. 3: An augmented graph with virtual nodes to address delays of the original graph.

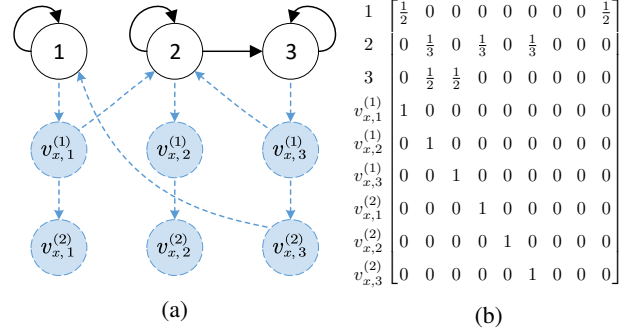


Fig. 4: (a) The topology of the x -type virtual nodes in the augmented graph at some time $t(k)$. Here node 1 uses the 2-steps delayed information $\tilde{\mathbf{x}}_3(k-3)$ and the latest information $\tilde{\mathbf{x}}_1(k-1)$ to compute $\mathbf{x}_1(k)$, and hence $(v_{x,3}^{(2)}, 1) \in \tilde{\mathcal{E}}(k)$. Node 2 uses $\tilde{\mathbf{x}}_2(k-1)$ and the 1-step delayed information $\tilde{\mathbf{x}}_1(k-2)$ and $\tilde{\mathbf{x}}_3(k-2)$ to compute $\mathbf{x}_2(k)$. Node 3 use the latest information $\tilde{\mathbf{x}}_2(k-1)$ and $\tilde{\mathbf{x}}_3(k-1)$ to compute $\mathbf{x}_3(k)$. (b) The corresponding row-stochastic matrix $\tilde{A}(k)$ in (7).

The topology of the y -type virtual nodes is similarly developed with reversed edge directions (c.f. Fig. 5(a)), which is the main motivation of using two types of virtual nodes. Firstly, edges $(v_{y,j}^{(1)}, j), (v_{y,j}^{(2)}, v_{y,j}^{(1)}), \dots,$ and $(v_{y,j}^{(nb)}, v_{y,j}^{(nb-1)})$ are always included in $\tilde{\mathcal{E}}(k)$ with the reversed directions of x -type nodes, see Fig. 3. Secondly, if $(i, j) \in \mathcal{E}$ in \mathcal{G} and $k \in \mathcal{T}_i$, then only one edge in edges $(i, v_{y,j}^{(1)}), (i, v_{y,j}^{(2)}), \dots, (i, v_{y,j}^{(nb)})$ and (i, j) is included in $\tilde{\mathcal{E}}(k)$, which also depends on the transmission delay of $\tilde{\mathbf{y}}_i$ sent from node i to node j . At time $t(k)$, suppose that node i sends $\mathbf{y}_i(k)$ to node j , which is received at $t(k+u)$ for $u > 1$, then $(i, v_{y,j}^{(u-1)}) \in \tilde{\mathcal{E}}(k)$ and the delay is u . Similarly, if there is no communication delay, i.e., $u = 1$, then $(i, j) \in \tilde{\mathcal{E}}(k)$. Fig. 5(a) illustrates such an augmented graph.

We provide a simple example to visualize the augmented graph approach. Consider that node i sends $\tilde{\mathbf{x}}_i(k)$ and $\tilde{\mathbf{y}}_i(k)$ to node j at time $t(k)$, and node j receives it at time $t(k+2)$, i.e., the delay is 1. In the augmented graph, this can be viewed as node i directly sends $\tilde{\mathbf{x}}_i(k)$ to the virtual node $v_{x,i}^{(1)}$, and sends $\tilde{\mathbf{y}}_i(k)$ to the virtual node $v_{y,j}^{(1)}$ at time $t(k)$. Nodes $v_{x,i}^{(1)}$ and $v_{y,j}^{(1)}$ respectively receive $\tilde{\mathbf{x}}_i(k)$ and $\tilde{\mathbf{y}}_i(k)$ at time $t(k+1)$, and immediately send them to node j at time $t(k+1)$. Finally,

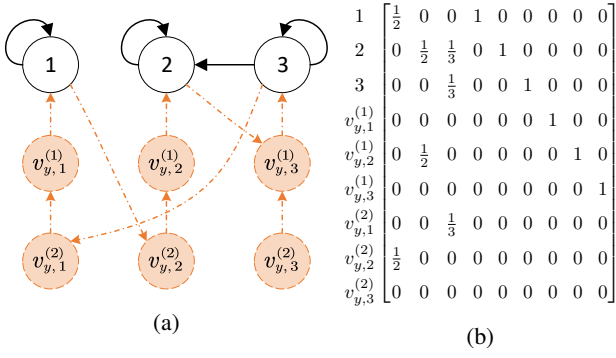


Fig. 5: (a) The topology of the y -type virtual nodes in the augmented graph at some time $t(k)$, which represents that node 1 sends $\tilde{y}_1(k)$ to node 2 and node 2 use it at $t(k+3)$ to compute $y_2(k+3)$. Other edges can be interpreted similarly. (b) The corresponding column-stochastic matrix $\tilde{B}(k)$ in (7).

node j receives $\tilde{x}_i(k)$ and $\tilde{y}_i(k)$ at time $t(k+2)$. Clearly, all non-virtual nodes in $\tilde{\mathcal{G}}$ receive the same information as that in \mathcal{G} and hence their updates appear to be synchronous and delay-free.

Under the time-varying augmented digraph, we are able to rewrite the APPG in a compact form.

B. A compact form of the APPG over the augmented digraph

Let $\mathbf{x}_i^{(u)}(k)$ and $\mathbf{y}_i^{(u)}(k)$ denote the states of virtual node $v_{x,i}^{(u)}$ and $v_{y,i}^{(u)}$ just after time $t(k)$, and $\tilde{n} = n(2b+1)$. Then, APPG can be rewritten in a compact form over $\tilde{\mathcal{G}}(k)$,

$$\begin{aligned}\tilde{X}(k+1) &= \tilde{A}(k)(\tilde{X}(k) - \Gamma I_k^a \tilde{Y}(k)), \\ \tilde{Y}(k+1) &= \tilde{B}(k)\tilde{Y}(k) + I_k^a(\nabla(k+1) - \nabla(k)) \\ &= \tilde{B}(k)\tilde{Y}(k) + \nabla(k+1) - \nabla(k)\end{aligned}\quad (7)$$

where

$$\begin{aligned}\tilde{X}(k) &= [X(k); X^{(1)}(k); \dots; X^{(b)}(k)] \in \mathbb{R}^{\tilde{n} \times m} \\ X^{(u)}(k) &= [\mathbf{x}_1^{(u)}(k), \dots, \mathbf{x}_n^{(u)}(k)]^\top \\ \tilde{Y}(k) &= [Y(k); Y^{(1)}(k); \dots; Y^{(b)}(k)] \in \mathbb{R}^{\tilde{n} \times m} \\ Y^{(u)}(k) &= [\mathbf{y}_1^{(u)}(k), \dots, \mathbf{y}_n^{(u)}(k)]^\top \\ \nabla(k) &= [\nabla \mathbf{f}(X(k)); \mathbf{0}_{(\tilde{n}-n) \times m}],\end{aligned}\quad (8)$$

the initial condition is $\tilde{X}(0) = [X(0); \mathbf{0}_{(\tilde{n}-n) \times m}]$, $\tilde{Y}(0) = \nabla(0)$, and $\tilde{A}(k), \tilde{B}(k), I_k^a \in \mathbb{R}^{\tilde{n} \times \tilde{n}}$ are

$$[\tilde{A}(k)]_{ij} = \begin{cases} \frac{1}{|\mathcal{X}_i(k)|}, & \text{if } i, v \in \mathcal{V}, j = nu + v, t(k+1) \in \mathcal{T}_i, \\ & \text{and node } i \text{ receives } \mathbf{x}_v(k-u) \text{ at } t(k+1) \\ 1, & \text{if } i \in \mathcal{V}, t(k+1) \notin \mathcal{T}_i \text{ and } j = i \\ 1, & \text{if } i \notin \mathcal{V} \text{ and } j = i - n \\ 0, & \text{otherwise,} \end{cases}$$

$$[\tilde{B}(k)]_{ji} = \begin{cases} \frac{1}{|\mathcal{N}_{out}^i|}, & \text{if } i, v \in \mathcal{V}, j = nu + v, t(k+1) \in \mathcal{T}_i, \\ & \text{and node } v \text{ receives } \mathbf{x}_i(k) \text{ at } t(k+u) \\ 1, & \text{if } i \in \mathcal{V}, t(k+1) \notin \mathcal{T}_i \text{ and } j = i \\ 1, & \text{if } i \notin \mathcal{V} \text{ and } j = i - n \\ 0, & \text{otherwise,} \end{cases}$$

$$[I_k^a]_{ij} = \begin{cases} 1, & \text{if } i = j, i \in \mathcal{V}, \text{ and } t(k+1) \in \mathcal{T}_i \\ 0, & \text{otherwise,} \end{cases}$$

where $|\mathcal{X}_i(k)|$ is the number of elements in the buffer \mathcal{X}_i at time $t(k+1)$.

An example of $\tilde{A}(k)$ and $\tilde{B}(k)$ is illustrated in Fig. 4(b) and Fig. 5(b), respectively. I_k^a is a diagonal matrix with its i -th diagonal element be 1 if node i is activated at time $t(k+1)$. The third equality in (7) follows from $\nabla(k+1) = \nabla(k)$ for any $i \in \{i | [I_k^a]_{ii} = 0\}$. An important fact is that $\tilde{A}(k)$ is a row-stochastic matrix and $\tilde{B}(k)$ is a column-stochastic matrix by the use of two types virtual nodes. Moreover,

$$\mathbf{1}_n^\top \tilde{Y}(k) = \mathbf{1}_n^\top \nabla(k) = \mathbf{1}_n^\top \nabla \mathbf{f}(X(k)) \quad (9)$$

which is obtained by left multiplying the second equality of (7) with $\mathbf{1}_n^\top$.

Note that (7) generates the same sequence of the states \mathbf{x}_i and \mathbf{y}_i as that of APPG. Hence, it is sufficient to study the convergence of $\tilde{X}(k)$ and $\tilde{Y}(k)$ in (7). To this end, we define

$$\begin{aligned}\Phi_t^A(k) &= \tilde{A}(k+t-1)\tilde{A}(k+t-2)\dots\tilde{A}(k+1)\tilde{A}(k) \\ \Phi_t^B(k) &= \tilde{B}(k+t-1)\tilde{B}(k+t-2)\dots\tilde{B}(k+1)\tilde{B}(k).\end{aligned}\quad (10)$$

where $k, t \in \mathbb{N}$, and we adopt the convention that $\Phi_t^A(k) = \Phi_0^B(k) = I$ and $\Phi_t^A(k) = \Phi_t^B(k) = 0$ for any $k \in \mathbb{N}$ and $t < 0$.

The following lemma states that $\Phi_t^A(k)$ and $\Phi_t^B(k)$ linearly converge to rank-one matrices.

Lemma 2: Under Assumptions 1, 2 and 3, the following statements are in force.

(a) There exist two stochastic vectors $\phi_t^A(k)$ and $\phi_t^B(k)$ such that

$$\|\Phi_t^A(k) - \mathbf{1}\phi_t^A(k)^\top\|_F \leq 2\rho^t, \quad \|\Phi_t^B(k) - \phi_t^B(k)\mathbf{1}^\top\|_F \leq 2\rho^t$$

for all $k, t \in \mathbb{N}$, where

$$\rho = (1 - \theta)^{\frac{1}{d_g b}} < 1, \quad \theta \geq \left(\frac{1}{\tilde{n}}\right)^{d_g b} \in (0, 1),$$

b is defined in Lemma 1(b), d_g is the diameter of \mathcal{G} and $\tilde{n} = n(2b+1)$.

(b) $\sum_{j=1}^{\tilde{n}} [\Phi_t^B(0)]_{ij} \geq n\theta, \forall i \in \mathcal{V}, t \in \mathbb{N}$.

Proof: In view of Lemma 1, both $\Phi_b^A(k)$ and $\Phi_b^B(k)$ are primitive for all k . Moreover, the minimum value of nonzero elements of $\tilde{A}(k)$ and $\tilde{B}(k)$ is greater than $1/\tilde{n}$. Then, the proof of the first part is similar with that of Lemma 5 in [41].

To prove (b), two cases are separately studied. If $t < d_g b$, then $[\Phi_t^B(0)]_{ii} \geq [\tilde{B}(t-1)]_{ii}[\tilde{B}(t-2)]_{ii}\dots[\tilde{B}(0)]_{ii} \geq (1/\tilde{n})^{d_g b-1} = \tilde{n}\theta \geq n\theta$, and hence the result is obtained.

If $t \geq d_g b$, it follows from a similar argument with the Lemma 2(b) in [41] that $[\Phi_{d_g b}(k)]_{ij} \geq \theta$ for all $i \in \mathcal{V}$ and $j \in \tilde{\mathcal{V}}$. Then,

$$\begin{aligned}[\Phi_{d_g b+1}(k-1)]_{ij} \\ = \sum_{u=1}^{\tilde{n}} [\Phi_{d_g b}(k)]_{iu} [\tilde{B}(k)]_{uj} \geq \theta \sum_{u=1}^{\tilde{n}} [\tilde{B}(k)]_{uj} \geq \theta.\end{aligned}$$

where the last inequality follows from the column-stochasticity of $\tilde{B}(k)$. The desired result is obtained by induction. \blacksquare

The following lemma is a direct result of Lemma 2, which specifies μ and \tilde{t} in Theorem 1.

Lemma 3: Under assumptions of Lemma 2, let $\mu = \frac{\theta^2}{2\tilde{n}} < 1$ and $\tilde{t} \in \mathbb{N}$ be a number such that $2\rho^{\tilde{t}} \leq \mu$, then for all $k \in \mathbb{N}$,

$$\|\Phi_{\tilde{t}}^A(k) - \mathbf{1}\phi_{\tilde{t}}^A(k)^\top\|_F \leq \mu, \quad \|\Phi_{\tilde{t}}^B(k) - \phi_{\tilde{t}}^B(k)\mathbf{1}^\top\|_F \leq \mu$$

Finally, we introduce the *absolute probability sequence* [42].

Lemma 4 (Theorem 4.2 in [42]): For a sequence of row-stochastic matrices $\{A(k)\}$, there exists a sequence of stochastic vectors $\{\pi(k)\}$ satisfying

$$\pi(k+1)^\top A(k) = \pi(k)^\top, \quad \forall k \in \mathbb{N}. \quad (11)$$

$\{\pi(k)\}$ is called an absolute probability sequence of $\{A(k)\}$.

In the sequel, we use $\pi(k) \in \mathbb{R}^{\tilde{n}}$ to denote an absolute probability sequence of $\tilde{A}(k)$, which implies that $\pi(k+t)^\top \Phi_{\tilde{t}}^A(k) = \pi(k)^\top, \forall k, t \in \mathbb{N}$.

VI. PROOF OF THEOREM 1 VIA LMIS

Under the augmented time-varying digraph, we are ready to prove Theorem 1.

A. Outline of the proof

As [19], for a nonnegative sequence $\{p(k)\}$, we define that

$$p^{\lambda,k} = \sup_{t \in \mathbb{N}, t \leq k} \frac{p(t)}{\lambda^t} \text{ and } \lambda \in (0, 1). \quad (12)$$

We call $\{p^{\lambda,k}\}$ the λ -sequence of $p(k)$. Clearly, if $p^{\lambda,k}$ is uniformly bounded by some constant c , then $p(k) \leq c\lambda^k$ for all k . Our method to prove Theorem 1 is to show the boundedness of $p^{\lambda,k}, k \in \mathbb{N}$ in (12) for some nonnegative sequences $p(k)$.

Under Assumptions 1, 2 and 3 and (7), the proof of Theorem 1 relies on four lemmas, whose proofs are given in next subsections.

Lemma 5: Let

$$Q(k) = I_{\tilde{n}} - \mathbf{1}_{\tilde{n}}\pi(k-1)^\top, \quad \|\tilde{X}(k)\|_Q = \|Q(k)\tilde{X}(k)\|_F,$$

and $\|\tilde{X}\|_Q^{\lambda,k}$ be the λ -sequence of $\|\tilde{X}(k)\|_Q$. If $\lambda^{\tilde{t}} \geq \frac{2\theta^2}{n}$, where \tilde{t} is defined in Lemma 3, then

$$\|\tilde{X}\|_Q^{\lambda,k} \leq \frac{4\tilde{n}\tilde{t}\tilde{\gamma}}{\theta^2} \|\tilde{Y}\|_F^{\lambda,k} + c_1 \quad (13)$$

where $\|\tilde{Y}\|_F^{\lambda,k}$ is the λ -sequence of $\|\tilde{Y}(k)\|_F$ and c_1 is a constant. \square

$\|\tilde{X}(k)\|_Q$ in Lemma 5 is a weighted difference among nodes' states $\mathbf{x}_i(k)$, and (13) bounds it by the gradient estimate $\|\tilde{Y}(k)\|_F$.

Lemma 6: Let

$$\begin{aligned} \mathbf{v}(k+1) &= \tilde{B}(k)\mathbf{v}(k), & \mathbf{v}(0) &= [\mathbf{1}_n; \mathbf{0}_{\tilde{n}-n}], \\ V(k) &= \text{diag}(\mathbf{v}(k)), & Y_V(k) &= V(k)^\dagger \tilde{Y}(k) \end{aligned}$$

where $V(k)^\dagger$ is the pseudo inverse of $V(k)$, i.e.,

$$[V(k)^\dagger]_{ij} = \begin{cases} 1/[V(k)]_{ii}, & \text{if } i = j \text{ and } [V(k)]_{ii} > 0, \\ 0, & \text{otherwise.} \end{cases}$$

Let $\tilde{I}(k) = V(k)V(k)^\dagger$, $\tilde{\mathbf{1}}(k) = \tilde{I}(k)\mathbf{1}_{\tilde{n}}$ and

$$S(k) = \tilde{I}(k) - \frac{1}{n}\tilde{\mathbf{1}}(k)\mathbf{v}(k)^\top, \quad \|Y_V(k)\|_S = \|S(k)Y_V(k)\|_F \quad (14)$$

Define the corresponding λ -sequence $\|Y_V\|_S^{\lambda,k}$ of $\{\|Y_V(k)\|_S\}$. If $\lambda^{\tilde{t}} > \frac{2\theta}{1+\theta}$, where \tilde{t} and μ are defined in Lemma 3, then

$$\|Y_V\|_S^{\lambda,k} \leq \frac{8\beta\tilde{n}\sqrt{\tilde{n}\tilde{t}}}{\theta^2 n} \left(\sqrt{n}\|\tilde{X}\|_Q^{\lambda,k} + \tilde{\gamma}\|\tilde{Y}\|_F^{\lambda,k} \right) + c_2 \quad (15)$$

where β is given in Assumption 1, $\theta, \tilde{t}, \tilde{n}$ are defined in Lemmas 2 and 3, and c_2 is given by (35). \square

Similarly, $\|Y_V(k)\|_S$ measures the differences between the weighted gradient estimates of different nodes, which is bounded by $\|\tilde{X}(k)\|_Q$ and $\|\tilde{Y}(k)\|_F$.

Lemma 7: Let

$$\mathbf{x}_\pi(k) = \pi(k)^\top \tilde{X}(k) \quad (16)$$

Define $\tilde{f}^{\lambda,k}$ be the λ -sequence of $\{\sqrt{f(\mathbf{x}_\pi(k)) - f^*}\}$. If $\tilde{\gamma} \leq \frac{1}{4nb\beta}$ and $\lambda^b \geq 1 - \frac{1}{8}\alpha\tilde{\gamma}\theta n$. Then,

$$\tilde{f}^{\lambda,k} \leq \frac{16b}{\alpha\theta\sqrt{\tilde{\gamma}\theta n}} \left(3n\beta\|\tilde{X}\|_Q^{\lambda,k} + \|Y_V\|_S^{\lambda,k} \right) + c_3 \quad (17)$$

where α, β are given in Assumption 1, b is defined in Lemma 1, θ is defined in Lemma 2, and c_3 is a constant. \square

Intuitively, $\mathbf{x}_\pi(k)$ is a weighted average of $\mathbf{x}_i(k), i \in \mathcal{V}$, and $f(\mathbf{x}_\pi(k)) - f^*$ is the optimality gap. Eq. (16) shows that the square root of the optimality gap can be bounded by $\|\tilde{X}\|_Q^{\lambda,k}$ and $\|Y_V\|_S^{\lambda,k}$.

Lemma 8: With the above-defined $\|\tilde{X}\|_Q^{\lambda,k}, \|Y_V\|_S^{\lambda,k}$ and $\tilde{f}^{\lambda,k}$, it holds that

$$\begin{aligned} \|\tilde{Y}\|_F^{\lambda,k} &\leq 2n(\sqrt{n}+1)\beta\sqrt{b}\|\tilde{X}\|_Q^{\lambda,k} + n\|Y_V\|_S^{\lambda,k} + \frac{2n\beta\sqrt{2nb}}{\sqrt{\alpha}}\tilde{f}^{\lambda,k} \end{aligned} \quad (18)$$

where β and b are given in Assumption 1 and Lemma 1, respectively. \square

Proof of Theorem 1: Note that λ defined in Theorem 1 satisfies all the conditions on λ of the above four lemmas and a sufficient small $\tilde{\gamma}$ will satisfy the condition of Lemma 7. Thus, (13), (15), (17) and (18) hold. Let

$$\mathbf{e}(k) = [\|\tilde{X}\|_Q^{\lambda,k}, \|Y_V\|_S^{\lambda,k}, \tilde{f}^{\lambda,k}, \|\tilde{Y}\|_F^{\lambda,k}]^\top, \quad c = [c_1, c_2, c_3, 0]^\top.$$

Combining (13), (15), (17), and (18), we obtain that for all $k \in \mathbb{N}$,

$$\mathbf{e}(k) \preceq M\mathbf{e}(k) + c \quad (19)$$

where \preceq is the element-wise inequality and M is a nonnegative matrix

$$M = \begin{bmatrix} 0 & 0 & 0 & \frac{4\tilde{n}\tilde{t}\tilde{\gamma}}{\theta^2} \\ \frac{8\beta\tilde{n}\sqrt{\tilde{n}\tilde{t}}}{\theta^2\sqrt{n}} & 0 & 0 & \frac{8\beta\tilde{n}\sqrt{\tilde{n}\tilde{t}\tilde{\gamma}}}{\theta^2 n} \\ \frac{48bn\beta}{\alpha\theta\sqrt{\tilde{\gamma}\theta n}} & \frac{16b}{\alpha\theta\sqrt{\tilde{\gamma}\theta n}} & 0 & 0 \\ 2n(\sqrt{n}+1)\beta\sqrt{b} & n & \frac{2n\beta\sqrt{2nb}}{\sqrt{\alpha}} & 0 \end{bmatrix}$$

It follows from (19) that if the spectral radius $\rho(M)$ of M is strictly less than 1, then $\|\tilde{X}\|_Q^{\lambda,k}, \|Y_V\|_S^{\lambda,k}$ and $\tilde{f}^{\lambda,k}$ are all bounded for all $k \in \mathbb{N}$.

Define a transformation matrix $T = \text{diag}([1, 1, \sqrt{\bar{\gamma}}, \sqrt{\bar{\gamma}}])$. Then, we can choose a small $\bar{\gamma}$ to make TMT^{-1} arbitrarily close to a strictly lower triangular matrix, and hence $\varrho(M) = \varrho(TMT^{-1}) < 1$ for a sufficiently small $\bar{\gamma}$ since the eigenvalues of a matrix are continuous functions on its elements. In fact, an upper bound of $\bar{\gamma}$ can be obtained by bounding $\|M^3\|_\infty$, which however can be conservative and thus we omit it here.

Define $\bar{c} := \frac{\max\{c_1, c_2, c_3\}}{1 - \varrho(M)} < \infty$, where c_1, c_2 and c_3 are given in (26), (35) and (41), respectively. It follows from (19) that $\|\tilde{X}\|_{\mathbb{Q}}^{\lambda, k} \leq \bar{c}$ and $\tilde{f}^{\lambda, k} \leq \bar{c}, \forall k$. We have

$$\begin{aligned} & \|\mathbf{x}_i(k) - \text{Proj}_{\mathcal{X}^*}(\mathbf{x}_\pi(k-1))\|_2 \\ & \leq \|\mathbf{x}_i(k) - \mathbf{x}_\pi(k-1)\|_2 + \|\mathbf{x}_\pi(k-1) - \text{Proj}_{\mathcal{X}^*}(\mathbf{x}_\pi(k-1))\|_2 \\ & \leq \|\tilde{X}(k)\|_{\mathbb{Q}} + \sqrt{2/\alpha} \sqrt{f(\mathbf{x}_\pi(k-1)) - f^*} \end{aligned}$$

where the last inequality used the equivalence between the Polyak-Łojasiewicz condition and the quadratic growth condition [40, Theorem 2], i.e., $f(\mathbf{x}) - f^* \geq \frac{\alpha}{2} \|\mathbf{x} - \text{Proj}_{\mathcal{X}^*}(\mathbf{x})\|_2^2, \forall \mathbf{x} \in \mathbb{R}^m$. Let $\mathbf{x}^*(k) = \text{Proj}_{\mathcal{X}^*}(\mathbf{x}_\pi(k-1))$ and $\|\mathbf{x}_i - \mathbf{x}^*\|_2^{\lambda, k}$ be the λ -sequence of $\{\|\mathbf{x}_i(k) - \mathbf{x}^*(k)\|_2\}$. We have

$$\|\mathbf{x}_i - \mathbf{x}^*\|_2^{\lambda, k} \leq \|\tilde{X}\|_{\mathbb{Q}}^{\lambda, k} + \sqrt{2/\alpha} \tilde{f}^{\lambda, k} \leq (1 + \sqrt{2/\alpha})\bar{c}, \forall i.$$

Combined with the boundedness of $\|\tilde{Y}\|_F^{\lambda, k}$, the result in Theorem 1 follows by the definition of λ -sequence. \blacksquare

B. Two useful propositions

We establish two important results in this subsection. The first one shows a property of λ -sequence and the second one recalls the contraction relation of gradient methods.

Proposition 1: Let $\{p(k)\}, \{q(k)\}$ be nonnegative sequences satisfying

$$p(t+j) \leq rp(t) + \sum_{i=0}^{j-1} q(t+i) \quad (20)$$

where $r \in [0, 1)$. If we choose λ such that $\lambda^j \in (r, 1)$, then the λ -sequences $p^{\lambda, k}$ and $q^{\lambda, k}$ in (12) satisfy

$$p^{\lambda, k} \leq \frac{j}{\lambda^j - r} q^{\lambda, k} + c_\lambda, \quad \forall k \in \mathbb{N},$$

where $c_\lambda = \frac{\lambda^j}{\lambda^j - r} \sum_{t=1}^m \lambda^{-t} p(t)$ is a constant. In particular, by letting $\lambda^j = \frac{2r}{1+r}$, we have

$$p^{\lambda, k} \leq \frac{2j}{r(1-r)} q^{\lambda, k} + c_\lambda, \quad \forall k \in \mathbb{N}, \quad (21)$$

Proof: It follows from (20) that

$$\begin{aligned} & \lambda^{-(t+j)} p(t+j) \\ & \leq \frac{r}{\lambda^j} \lambda^{-t} p(t) + \sum_{i=0}^{j-1} \frac{1}{\lambda^{j-i}} \lambda^{-(t+i)} q(t+i), \quad \forall t = 1, \dots, k. \end{aligned}$$

This gives k inequalities by selecting $t = 1, \dots, k$. On the other hand, we have $\lambda^{-t} p(t) \leq \lambda^{-t} p(t)$, which gives another j inequalities by selecting $t = 1, \dots, j$. Take the maximum

on both sides of these $k+j$ inequalities and use the definition of λ -sequence, we obtain

$$\begin{aligned} p^{\lambda, k+j} & \leq \frac{r}{\lambda^j} p^{\lambda, k} + \max \left\{ q^{\lambda, k} \sum_{i=0}^{j-1} \frac{1}{\lambda^{j-i}}, \max_{t=1, \dots, j} \lambda^{-t} p(t) \right\} \\ & \leq \frac{r}{\lambda^j} p^{\lambda, k+j} + q^{\lambda, k+j} \sum_{i=0}^{j-1} \frac{1}{\lambda^{j-i}} + \sum_{t=1}^j \lambda^{-t} p(t) \end{aligned} \quad (22)$$

If $\lambda^j \in (r, 1)$, then (22) implies

$$\begin{aligned} p^{\lambda, k+j} & \leq \frac{\lambda^j \sum_{i=0}^{j-1} \frac{1}{\lambda^{j-i}}}{\lambda^j - r} q^{\lambda, k+j} + \frac{\lambda^j}{\lambda^j - r} \sum_{t=1}^j \lambda^{-t} p(t) \\ & = \frac{1 - \lambda^j}{(\lambda^j - r)(1 - \lambda)} q^{\lambda, k+j} + \frac{\lambda^j}{\lambda^j - r} \sum_{t=1}^j \lambda^{-t} p(t) \\ & \leq \frac{j}{\lambda^j - r} q^{\lambda, k+j} + \frac{\lambda^j}{\lambda^j - r} \sum_{t=1}^j \lambda^{-t} p(t) \end{aligned}$$

for all $k+j \in \mathbb{N}$, where we have used that $1 - \lambda^j \leq j(1 - \lambda)$. The result is obtained immediately. For $\lambda^j \in (\frac{2r}{1+r}, 1)$, we have $\lambda^j - r \geq r(1 - r)/2$, and hence (21) follows. \blacksquare

We introduce another important property of λ -sequence. For any nonnegative sequences $\{p(k)\}, \{q(k)\}$, letting $r(k) = p(k) + q(k)$, it holds that $r^{\lambda, k} \leq p^{\lambda, k} + q^{\lambda, k}$, which can be easily checked by definition.

The following proposition shows the convergence rate of a perturbed gradient descent method for minimizing functions satisfying the PL condition. As a special case, it recovers the linear convergence rate of the standard gradient descent method.

Proposition 2: Suppose that f is β -Lipschitz smooth and satisfies the Polyak-Łojasiewicz condition in Assumption 1(c). Let $\eta \in (0, \frac{1}{2\beta})$, $\sigma = 1 - \alpha\eta(1 - 2\eta\beta) < 1$, and $\mathbf{x}^+ = \mathbf{x} - \eta\nabla f(\mathbf{x}) + \varepsilon$. Then

$$f(\mathbf{x}^+) - f^* \leq \sigma(f(\mathbf{x}) - f^*) + \left(\frac{2}{\eta} + \beta\right) \|\varepsilon\|_2^2, \quad \forall \mathbf{x} \in \mathbb{R}^n.$$

Proof: It follows from the β -Lipschitz smoothness that

$$\begin{aligned} & f(\mathbf{x}^+) \\ & \leq f(\mathbf{x}) + \nabla f(\mathbf{x})^\top (-\eta\nabla f(\mathbf{x}) + \varepsilon) + \frac{\beta}{2} \|\eta\nabla f(\mathbf{x}) + \varepsilon\|_2^2 \\ & \leq f(\mathbf{x}) - \eta\|\nabla f(\mathbf{x})\|_2^2 + \frac{\eta}{2} \|\nabla f(\mathbf{x})\|_2^2 + \frac{2}{\eta} \|\varepsilon\|_2^2 \\ & \quad + \beta\eta^2 \|\nabla f(\mathbf{x})\|_2^2 + \beta\|\varepsilon\|_2^2 \\ & \leq f(\mathbf{x}) - \eta\left(\frac{1}{2} - \eta\beta\right) \|\nabla f(\mathbf{x})\|_2^2 + \left(\frac{2}{\eta} + \beta\right) \|\varepsilon\|_2^2 \end{aligned}$$

Applying the Polyak-Łojasiewicz inequality on $\|\nabla f(\mathbf{x})\|_2^2$ implies the desired result:

$$\begin{aligned} & f(\mathbf{x}^+) - f^* \\ & \leq f(\mathbf{x}) - f^* - 2\alpha\eta\left(\frac{1}{2} - \eta\beta\right)(f(\mathbf{x}) - f^*) + \left(\frac{2}{\eta} + \beta\right) \|\varepsilon\|_2^2 \\ & \leq (1 - \alpha\eta(1 - 2\eta\beta))(f(\mathbf{x}) - f^*) + \left(\frac{2}{\eta} + \beta\right) \|\varepsilon\|_2^2. \end{aligned}$$

\blacksquare

We end this subsection with two inequalities which will be frequently used later. For any $A, B \in \mathbb{R}^{n \times n}$,

$$\|AB\|_F \leq \|A\|_2 \|B\|_F, \quad \|A\|_2 \leq \sqrt{\|A\|_\infty \|A\|_1},$$

and $\|A\|_2 \leq \|A\|_F \leq \sqrt{n}$ for any row-stochastic matrix A .

C. Proof of Lemma 5

Let \tilde{t} be defined as in Lemma 3. It follows from (7) and (10) that

$$\begin{aligned} \|\tilde{X}(k + \tilde{t})\|_Q &= \|Q(k + \tilde{t})\tilde{X}(k + \tilde{t})\|_F \\ &\leq \|Q(k + \tilde{t})\Phi_{\tilde{t}}^A(k)\tilde{X}(k)\|_F \\ &\quad + \sum_{t=0}^{\tilde{t}-1} \|Q(k + \tilde{t})\Phi_{\tilde{t}-t}^A(k+t)\Gamma I_{k+t}^a \tilde{Y}(k+t)\|_F \end{aligned} \quad (23)$$

By the stochastic vector $\phi_{\tilde{t}}^A(k)$ in Lemma 3, (23) implies that

$$\begin{aligned} \|\tilde{X}(k + \tilde{t})\|_Q &\leq \|Q(k + \tilde{t})(\Phi_{\tilde{t}}^A(k) - \mathbf{1}\phi_{\tilde{t}-1}^A(k)^\top)Q(k)\tilde{X}(k)\|_F \\ &\quad + \gamma \sum_{t=0}^{\tilde{t}-1} \|Q(k + \tilde{t})\|_2 \|\Phi_{\tilde{t}-t}^A(k+t)\|_2 \|I_{k+t}^a \tilde{Y}(k+t)\|_F \\ &\leq \|Q(k + \tilde{t})\|_2 \|\Phi_{\tilde{t}}^A(k) - \mathbf{1}\phi_{\tilde{t}}^A(k)^\top\|_F \|Q(k)\tilde{X}(k)\|_F \\ &\quad + 2\gamma \sum_{t=0}^{\tilde{t}-1} \|\Phi_{\tilde{t}-t}^A(k+t)\|_2 \|\tilde{Y}(k+t)\|_F \\ &\leq \sqrt{\tilde{n}}\mu \|\tilde{X}(k)\|_Q + 2\gamma\sqrt{\tilde{n}} \sum_{t=0}^{\tilde{t}-1} \|\tilde{Y}(k+t)\|_F \end{aligned} \quad (24)$$

where $\mu = \frac{\theta^2}{2\tilde{n}} < 1$ is given in Lemma 3, the first inequality used the fact that $\|Q(k)\|_2 \leq \sqrt{\tilde{n}}, \forall k, \Phi_{\tilde{t}}^A(k)$ is row-stochastic and

$$\begin{aligned} &Q(k+t)(A - \mathbf{1}\pi(k-1)^\top)Q(k) \\ &= Q(k+t)AQ(k) - Q(k+t)\mathbf{1}\pi(k-1)^\top Q(k) \\ &= Q(k+t)(A - \mathbf{1}\tilde{n}\pi(k-1)^\top) \\ &\quad - Q(k+t)(\mathbf{1}\tilde{n}\pi(k-1)^\top - \mathbf{1}\tilde{n}\pi(k-1)^\top) \\ &= Q(k+t)A - Q(k+t)\mathbf{1}\tilde{n}\pi(k-1)^\top = Q(k+t)A \end{aligned} \quad (25)$$

for any row-stochastic matrix A and $k \in \mathbb{N}$. The last inequality of (24) follows from Lemma 3 and $\|\Phi_{\tilde{t}}^A(k)\|_2 \leq \sqrt{\tilde{n}}$.

Note that $\mu < 1/2$. In view of Proposition 1 and (24), we obtain that

$$\|\tilde{X}\|_Q^{\lambda, k} \leq \frac{2\gamma\sqrt{\tilde{n}t}}{\sqrt{\tilde{n}}\mu(1 - \sqrt{\tilde{n}}\mu)} \|\tilde{Y}\|_Q^{\lambda, k} + c_1$$

for any $\lambda^{\tilde{t}} > \frac{2\sqrt{\tilde{n}}\mu}{1 + \sqrt{\tilde{n}}\mu}$, where

$$c_1 = \frac{2\gamma\sqrt{\tilde{n}}\lambda^{\tilde{t}}}{\lambda^{\tilde{t}} - \sqrt{\tilde{n}}\mu} \sum_{t=1}^{\tilde{t}} \lambda^{-t} \|\tilde{X}(t)\|_Q. \quad (26)$$

The desired result is obtained by setting $\mu = \frac{\theta^2}{2\tilde{n}}$. ■

D. Proof of Lemma 6

Let $\mathbf{v}(k) = [v_1(k), \dots, v_{\tilde{n}}(k)]^\top$ and $\mathcal{I}_V(k) = \{i | v_i(k) = [V(k)]_{ii} = 0\}$. Note that $v_i(k) \geq n\theta$ for all $i \in \mathcal{V}, k \in \mathbb{N}$ from Lemma 2(b). It can be shown that the i -th row of $\tilde{Y}(k)$ is $\mathbf{0}_m^\top$ for all $i \in \mathcal{I}_V(k)$, and thus $\tilde{Y}(k) = V(k)Y_V(k)$.

Let $R(k) = \nabla(k+1) - \nabla(k)$. It then follows from (7) that

$$Y_V(k+1) = \tilde{B}_V(k)Y_V(k) + V(k+1)^\dagger R(k) \quad (27)$$

where $\tilde{B}_V(k) = V(k+1)^\dagger \tilde{B}(k)V(k)$ and one can prove that each row except the i -th ($i \in \mathcal{I}_V(k)$) row of $\tilde{B}_V(k)$ has row sum 1 using similar arguments as in Lemma 4 of [43] and [19]. Using the definition of $\nabla(k)$ in (8) and Assumption 1, we have

$$\begin{aligned} \|R(k)\|_F &= \|\nabla(k+1) - \nabla(k)\|_F \leq \beta \|X(k+1) - X(k)\|_F \\ &\leq \beta \|\tilde{X}(k+1) - \tilde{X}(k)\|_F \end{aligned} \quad (28)$$

where we have used Assumption 1.

Notice that

$$\begin{aligned} \|\tilde{X}(k+1) - \tilde{X}(k)\|_F &= \|\tilde{A}(k)\tilde{X}(k) - \Gamma I_k^a \tilde{Y}(k) - \tilde{X}(k)\|_F \\ &\leq \|(\tilde{A}(k) - I)Q(k)\tilde{X}(k)\|_F + \gamma \|\tilde{Y}(k)\|_F \\ &\leq 2\sqrt{\tilde{n}} \|\tilde{X}(k)\|_Q + \gamma \|\tilde{Y}(k)\|_F \end{aligned} \quad (29)$$

where the second inequality follows from the row-stochasticity of $\tilde{A}(k)$, and the last inequality is from that $\|\tilde{A}(k) - I\|_2 \leq \|\tilde{A}(k)\|_2 + \|I\|_2 \leq \sqrt{\|\tilde{A}(k)\|_1} + 1 \leq \sqrt{\tilde{n}} + 1 \leq 2\sqrt{\tilde{n}}$. By Combining (28) and (29), we obtain

$$\|R(k)\|_F \leq 2\beta\sqrt{\tilde{n}} \|\tilde{X}(k)\|_Q + \beta\gamma \|\tilde{Y}(k)\|_F \quad (30)$$

To analyze the sequence $\{Y_V(k)\}$, we define

$$\begin{aligned} \tilde{\Phi}_t(k) &:= \tilde{B}_V(k+t-1)\tilde{B}_V(k+t-2)\cdots\tilde{B}_V(k+1)\tilde{B}_V(k) \\ &= V(k+t)^\dagger \left(\prod_{l=t-1}^1 \tilde{B}(k+l)\tilde{I}(k+l) \right) \tilde{B}(k)V(k) \\ &= V(k+t)^\dagger \Phi_t^B(k)V(k). \end{aligned} \quad (31)$$

where

$$[\tilde{I}(k)]_{ij} = [V(k)V(k)^\dagger]_{ij} = \begin{cases} 1, & \text{if } i = j, i \notin \mathcal{I}_V(k), \\ 0, & \text{otherwise.} \end{cases}$$

and the last equality follows from that $\tilde{I}(k+1)\tilde{B}(k)V(k) = \tilde{B}(k)V(k), \forall k \in \mathbb{N}$, where we used the fact that $[\tilde{B}(k)V(k)\mathbf{1}_{\tilde{n}}] = v_i(k+1) = 0$ for any $i \in \mathcal{I}_V(k+1)$, and thus the i -th row of $\tilde{B}(k)V(k)$ is $\mathbf{0}_m^\top$.

We know from Lemma 2 and Lemma 3 that $\Phi_t^B(k)$ can be written as

$$\Phi_t^B(k) = \phi_t^B(k)\mathbf{1}^\top + \Delta\Phi_t(k) \quad (32)$$

where $\|\Delta\Phi_t(k)\|_F \leq 2\rho^t$ and $\|\Delta\Phi_{\tilde{t}}(k)\|_F \leq \mu < 1$. Hence,

$$\begin{aligned} \mathbf{v}(k+t) &= \Phi_t^B(k)\mathbf{v}(k) = \phi_t^B(k)\mathbf{1}^\top \mathbf{v}(k) + \Delta\Phi_t(k)\mathbf{v}(k) \\ &= \phi_t^B(k)\mathbf{1}^\top \mathbf{v}(0) + \Delta\Phi_t(k)\mathbf{v}(k) = n\phi_t^B(k) + \Delta\Phi_t(k)\mathbf{v}(k) \end{aligned}$$

which implies that

$$\phi_t^B(k) = \frac{1}{n} (\mathbf{v}(k+t) - \Delta\Phi_t(k)\mathbf{v}(k)). \quad (33)$$

It then follows from (31), (32) and (33) that

$$\begin{aligned}\tilde{\Phi}_t(k) &= \frac{1}{n}V(k+t)^\dagger \mathbf{v}(k+t) \mathbf{1}_n^\top V(k) \\ &\quad + V(k+t)^\dagger \Delta \Phi_t(k) \left(I - \frac{1}{n} \mathbf{v}(k) \mathbf{1}_n^\top \right) V(k) \\ &= \frac{1}{n} \tilde{\mathbf{1}}(k+t) \mathbf{v}(k)^\top + C_t(k)\end{aligned}$$

where $\tilde{\mathbf{1}}(k) = \tilde{I}(k) \mathbf{1}$, $C_t(k) = V(k+t)^\dagger \Delta \Phi_t(k) \left(I - \frac{1}{n} \mathbf{v}(k) \mathbf{1}_n^\top \right) V(k)$ and

$$\begin{aligned}\|C_t(k)\|_F &\leq \|V(k+t)^\dagger\|_2 \|\Delta \Phi_t(k)\|_F \left\| \left(I - \frac{1}{n} \mathbf{v}(k) \mathbf{1}_n^\top \right) V(k) \right\|_F \\ &< \theta^{-1} \mu n.\end{aligned}$$

where we used the fact that all entries of $V(k)^\dagger$ are less than θ^{-1} by Lemma 2. Thus

$$\left\| \tilde{\Phi}_t(k) - \frac{1}{n} \tilde{\mathbf{1}}(k+t) \mathbf{v}(k)^\top \right\|_F \leq \theta^{-1} \mu n \leq \frac{\theta}{2} < \frac{1}{2}.$$

Now we turn to the sequence $\{Y_V(k)\}$. It follows from (14) and (27) that

$$\begin{aligned}\|Y_V(k+\tilde{t})\|_S &= \|S(k+\tilde{t})Y_V(k+\tilde{t})\|_F \\ &\leq \|S(k+\tilde{t})\tilde{\Phi}_t(k)Y_V(k)\|_F \\ &\quad + \sum_{t=1}^{\tilde{t}} \|S(k+t)\tilde{\Phi}_{\tilde{t}-t}(k+t)V(k+t)^\dagger R(k+t-1)\|_F \\ &\leq \|S(k+\tilde{t})\tilde{\Phi}_t(k)Y_V(k)\|_F \\ &\quad + \sum_{t=1}^{\tilde{t}} \|S(k+t)V(k+t+1)^\dagger \Phi_{\tilde{t}-t}^B(k+t)R(k+t-1)\|_F\end{aligned}\tag{34}$$

Similar to (25), we have $S(k+\tilde{t})\tilde{\Phi}_t(k) = S(k+\tilde{t})\left(\tilde{\Phi}_t(k) - \frac{1}{n}\tilde{\mathbf{1}}(k+t)\mathbf{v}(k)^\top\right)S(k)$. Following a similar argument as in (24) and using (30), equation (34) implies that

$$\begin{aligned}\|Y_V(k+\tilde{t})\|_S &\leq 2\theta^{-1}\mu n \|Y_V(k)\|_S + 2\sqrt{\tilde{n}} \sum_{t=0}^{\tilde{t}-1} \|V(k+t+2)^\dagger R(k+t)\|_F \\ &\leq 2\theta^{-1}\mu n \|Y_V(k)\|_S \\ &\quad + 2\beta\theta^{-1}\sqrt{\tilde{n}} \sum_{t=0}^{\tilde{t}-1} \left(2\sqrt{\tilde{n}} \|\tilde{X}(k+t)\|_Q + \tilde{\gamma} \|\tilde{Y}(k+t)\|_F \right)\end{aligned}$$

where we used the relation $\|V(k)^\dagger\|_2 \leq \theta^{-1}, \forall k$ and (30).

By Proposition 1, we have for any $\lambda^{\tilde{t}} > (1 + 2\theta^{-1}\mu n)/2$ that

$$\begin{aligned}\|Y_V\|_S^{\lambda,k} &\leq \frac{2\beta\theta^{-1}n(1-\lambda^{\tilde{t}})}{(\lambda^{\tilde{t}} - 2\theta^{-1}\mu n)(1-\lambda)} \|\tilde{X}\|_Q^{\lambda,k} \\ &\quad + \frac{2\tilde{\gamma}\beta\theta^{-1}\sqrt{\tilde{n}}(1-\lambda^{\tilde{t}})}{(\lambda^{\tilde{t}} - 2\theta^{-1}\mu n)(1-\lambda)} \|\tilde{Y}\|_F^{\lambda,k} + c'_2 \\ &\leq \frac{2\beta\theta^{-1}\sqrt{\tilde{n}t}}{\theta^{-1}\mu n(1-2\theta^{-1}\mu n)} \left(\sqrt{\tilde{n}} \|\tilde{X}\|_Q^{\lambda,k} + \tilde{\gamma} \|\tilde{Y}\|_F^{\lambda,k} \right) + c'_2\end{aligned}$$

where

$$c_2 = \frac{2\beta\theta^{-1}\sqrt{\tilde{n}}\lambda^{\tilde{t}}}{\lambda^{\tilde{t}} - 2\theta^{-1}\mu n} \sum_{t=1}^{\tilde{t}} \lambda^{-t} \left(\sqrt{\tilde{n}} \|\tilde{X}(t)\|_Q + \tilde{\gamma} \|\tilde{X}(t)\|_Q \right)\tag{35}$$

The desired result is obtained by setting $\mu = \frac{\theta^2}{2\tilde{n}}$. ■

E. Proof of Lemma 7

It follows from (7), (11) and (16) that

$$\begin{aligned}\mathbf{x}_\pi(k+b) &= \pi(k+b)^\top \tilde{X}(k+b) \\ &= \pi(k+b)^\top \Phi_b^A(k) \tilde{X}(k) \\ &\quad - \pi(k+b)^\top \sum_{t=0}^{b-1} \Phi_{b-t}^A(k+t+1) I_{k+t}^a \Gamma V(k+t) Y_V(k+t) \\ &= \pi(k)^\top \tilde{X}(k) - \frac{1}{n} \sum_{t=0}^{b-1} \eta_k(t) \mathbf{1}_n^\top \nabla(k+t) \\ &\quad - \sum_{t=0}^{b-1} \mathbf{r}_k(t) \left(Y_V(k+t) - \frac{1}{n} \tilde{\mathbf{1}}(k+t) \mathbf{1}_n^\top \nabla(k+t) \right)\end{aligned}\tag{36}$$

where $V(k)$ and $\tilde{\mathbf{1}}(k)$ are defined in Lemma 6, $\mathbf{r}_k(t) = \pi(k+b)^\top \Phi_{b-t}^A(k+t+1) I_{k+t}^a \Gamma V(k+t)$ and $\eta_k(t) = \mathbf{r}_k(t) \tilde{\mathbf{1}}(k+t)$. We have

$$\eta_k(t) \leq \eta := \tilde{\gamma} n, \quad \forall k, t \in \mathbb{N},\tag{37a}$$

$$\begin{aligned}\sum_{t=0}^{b-1} \eta_k(t) &\geq \pi(k+b)^\top \sum_{t=0}^{b-1} \Phi_{b-t}^A(k+t+1) I_{k+t}^a \Gamma \mathbf{v}(k+t) \\ &\geq \underline{\gamma} \theta n,\end{aligned}\tag{37b}$$

$$\sum_{t=0}^{b-1} \eta_k(t) \leq b\eta \leq \tilde{\gamma} n b < \frac{1}{4\beta}, \quad \forall k.\tag{37c}$$

where we used the relation $v_i(k) \geq n\theta, \forall i \in \mathcal{V}, k \in \mathbb{N}$ from Lemma 2(b) and the fact that the sum of any row of $\sum_{t=0}^{b-1} \Phi_{b-t}^A(k+t+1) I_{k+t}^a$ is not smaller than 1 to obtain (37b).

By introducing an auxiliary term $\sum_{t=0}^{b-1} \eta_k(t) \nabla f(\mathbf{x}_\pi(k))^\top$, Eq. (36) becomes

$$\begin{aligned}\mathbf{x}_\pi(k+b) &= \mathbf{x}_\pi(k) - \sum_{t=0}^{b-1} \eta_k(t) \nabla f(\mathbf{x}_\pi(k))^\top \\ &\quad + \underbrace{\sum_{t=0}^{b-1} \eta_k(t) \left(\nabla f(\mathbf{x}_\pi(k))^\top - \frac{1}{n} \mathbf{1}_n^\top \nabla(k+t) \right)}_{\mathbf{h}(k)} \\ &\quad - \sum_{t=0}^{b-1} \mathbf{r}_k(t) \left(Y_V(k+t) - \frac{1}{n} \tilde{\mathbf{1}}(k+t) \mathbf{v}(k+t)^\top Y_V(k+t) \right)\end{aligned}\tag{38}$$

where we have used the relation $\mathbf{1}_n^\top \nabla(k) = \mathbf{1}_n^\top \tilde{Y}(k) = \mathbf{v}(k)^\top Y_V(k)$ in (9).

We now bound $\mathbf{h}(k)$ in (38). Recall that $\nabla f(\mathbf{x}) = \mathbf{1}_n^\top \nabla f(\mathbf{1}_n \mathbf{x}^\top), \forall \mathbf{x} \in \mathbb{R}^m$ and $\mathbf{1}_n^\top \nabla(k) = [\mathbf{1}_n; \mathbf{0}]^\top \nabla(k) = \mathbf{1}_n^\top \nabla f(X(k)), \forall k$. Let $\tilde{\mathbf{1}} = [\mathbf{1}_n; \mathbf{0}_{\tilde{n}-n}]$, we have

$$\|\mathbf{h}(k)\|_F\tag{39}$$

$$\begin{aligned}
&= \left\| \sum_{t=0}^{b-1} \eta_k(t) (\mathbf{1}_n^\top \nabla \mathbf{f}(\mathbf{1}_n \mathbf{x}_\pi(k)) - \mathbf{1}_n^\top \nabla \mathbf{f}(X(k+t))) \right\|_F \\
&\leq \sqrt{n} \beta \eta \sum_{t=0}^{b-1} \|\mathbf{1}_n \mathbf{x}_\pi(k) - X(k+t)\|_F \\
&\leq \sqrt{n} \beta \eta \left(\sum_{t=0}^{b-1} \left\| \tilde{\mathbf{1}}_{\mathbf{x}_\pi(k)}^\top - \tilde{\mathbf{1}}_{\pi_{k+t-1}}^\top \tilde{X}(k+t) \right\|_F + \right. \\
&\quad \left. \sum_{t=0}^{b-1} \left\| \tilde{\mathbf{1}}_{\pi_{k+t-1}}^\top \tilde{X}(k+t) - \begin{bmatrix} I_n & \mathbf{0} \\ \mathbf{0} & \mathbf{0} \end{bmatrix} \tilde{X}(k+t) \right\|_F \right) \\
&\leq \sqrt{n} \beta \eta \left(\sum_{t=0}^{b-1} \left\| \tilde{\mathbf{1}}(\pi_{k-1} - \pi_{k+t-1})^\top Q(k+t) \tilde{X}(k+t) \right\|_F \right. \\
&\quad \left. + \sum_{t=0}^{b-1} \left\| \begin{bmatrix} I_n & \mathbf{0} \\ \mathbf{0} & \mathbf{0} \end{bmatrix} (\mathbf{1}_{\tilde{n}} \pi_{k+t-1}^\top \tilde{X}(k+t) - \tilde{X}(k+t)) \right\|_F \right) \\
&\leq 3n\beta\eta \sum_{t=0}^{b-1} \|\tilde{X}(k+t)\|_Q \leq 3\bar{\gamma}n^2\beta \sum_{t=0}^{b-1} \|\tilde{X}(k+t)\|_Q
\end{aligned}$$

where we defined $\pi_k := \pi(k)$ to save space.

By combining (38) and (39), we obtain

$$\begin{aligned}
\mathbf{x}_\pi(k+b) &= \mathbf{x}_\pi(k) - \sum_{t=0}^{b-1} \eta_k(t) \nabla f(\mathbf{x}_\pi(k))^\top + \mathbf{h}(k) \\
&\quad - \sum_{t=0}^{b-1} \mathbf{r}_k(t) S(k+t) Y_V(k+t).
\end{aligned}$$

Then, Proposition 2 implies that

$$\begin{aligned}
f(\mathbf{x}_\pi(k+b)) - f^* &\leq \sigma^2 (f(\mathbf{x}_\pi(k)) - f^*) \\
&\quad + \left(\frac{2}{\sum_{t=0}^{b-1} \eta_k(t)} + \beta \right) \left\| \mathbf{h}(k) - \sum_{t=0}^{b-1} \mathbf{r}_k(t) S(k+t) Y_V(k+t) \right\|_2^2 \\
\text{where } \sigma &= \sqrt{1 - \alpha \sum_{t=1}^b \eta_k(t) (1 - 2\beta \sum_{t=1}^b \eta_k(t))}, \text{ and we} \\
\text{have } \sigma &\leq 1 - \frac{1}{2} \alpha \bar{\gamma} \theta n (1 - 2\beta \bar{\gamma} b n) < 1 - \frac{1}{4} \alpha \bar{\gamma} \theta n < 1 \text{ using} \\
\sqrt{1-a} &\leq 1 - \frac{1}{2} a, \forall a \in (0, 1), \bar{\gamma} n \beta b \leq 0.25, \text{ and (37). Using} \\
\sqrt{a+b} &\leq \sqrt{a} + \sqrt{b}, \text{ we obtain} \\
\tilde{f}(k+b) &= \sqrt{f(\mathbf{x}_\pi(k+b)) - f^*} \leq \sigma \sqrt{f(\mathbf{x}_\pi(k)) - f^*} \\
&\quad + \left(\sqrt{\beta} + \frac{\sqrt{2}}{\sqrt{\bar{\gamma} \theta n}} \right) \left(\|\mathbf{h}(k)\|_F + \sum_{t=0}^{b-1} \|\mathbf{r}_k(t)\|_2 \|Y_V(k+t)\|_S \right) \\
&\leq \sigma \tilde{f}(k) + \left(\bar{\gamma} n \sqrt{\beta} + \frac{\sqrt{2\bar{\gamma} n}}{\sqrt{\theta}} \right) 3n\beta \sum_{t=0}^{b-1} \|\tilde{X}(k+t)\|_Q \\
&\quad + \left(\bar{\gamma} n \sqrt{\beta} + \frac{\sqrt{2\bar{\gamma} n}}{\sqrt{\theta}} \right) \sum_{t=0}^{b-1} \|Y_V(k+t)\|_S \\
&\leq \frac{2\sqrt{\bar{\gamma} n}}{\sqrt{\theta}} 3n\beta \sum_{t=0}^{b-1} \|\tilde{X}(k+t)\|_Q + \frac{2\sqrt{\bar{\gamma} n}}{\sqrt{\theta}} \sum_{t=0}^{b-1} \|Y_V(k+t)\|_S \\
&\quad + \sigma \tilde{f}(k)
\end{aligned} \tag{40}$$

where the first two inequalities follow from (37), (39), and $\|\mathbf{r}_k(t)\|_2 \leq \bar{\gamma} n, \forall k, t$. The last inequality follows from $\sqrt{\bar{\gamma} n \beta \theta} \leq \sqrt{\bar{\gamma} n \beta} \leq 0.5$.

Use the condition that $\lambda^b > 1 - \frac{1}{8} \alpha \bar{\gamma} \theta n$, $\sigma < 1 - \frac{1}{4} \alpha \bar{\gamma} \theta n$ and Proposition 1, we obtain from (40) that

$$\begin{aligned}
\tilde{f}^{\lambda, k} &\leq \frac{2\sqrt{\bar{\gamma} n b} \left(3n\beta \|\tilde{X}\|_Q^{\lambda, k} + \|Y_V\|_S^{\lambda, k} \right)}{(\lambda^b - (1 - \frac{1}{4} \alpha \bar{\gamma} \theta n)) \sqrt{\theta}} + c_3 \\
&\leq \frac{16b}{\alpha \theta \sqrt{\bar{\gamma} \theta n}} \left(3n\beta \|\tilde{X}\|_Q^{\lambda, k} + \|Y_V\|_S^{\lambda, k} \right) + c_3
\end{aligned}$$

where

$$c_3 = \frac{16}{\alpha \theta \sqrt{\bar{\gamma} \theta n}} \sum_{t=0}^{b-1} \lambda^{-t} \left(3n\beta \|\tilde{X}(t)\|_Q + \|Y_V(t)\|_S \right). \tag{41}$$

F. Proof of Lemma 8

Since

$$\begin{aligned}
\tilde{Y}(k) &= V(k) Y_V(k) \\
&= V(k) S(k) Y_V(k) + \frac{1}{n} V(k) \tilde{\mathbf{1}}(k) \mathbf{v}(k)^\top Y_V(k)
\end{aligned}$$

we have

$$\begin{aligned}
\|\tilde{Y}(k)\|_F &\leq \|V(k)\|_2 \left(\|Y_V(k)\|_S + \left\| \frac{1}{n} \tilde{\mathbf{1}}(k) \mathbf{v}(k)^\top Y_V(k) \right\|_F \right) \\
&\leq n \|Y_V(k)\|_S + \left\| \tilde{\mathbf{1}}(k) \mathbf{1}_n^\top \nabla(k) \right\|_F.
\end{aligned} \tag{42}$$

Note that

$$\|\tilde{\mathbf{1}}(k) \mathbf{1}_n^\top \nabla(k)\|_F = \left\| \tilde{\mathbf{1}}(k) (\mathbf{1}_n^\top \nabla \mathbf{f}(X(k)) - \mathbf{1}_n^\top \nabla \mathbf{f}(\mathbf{1}_n (\mathbf{x}^*)^\top)) \right\|_F \tag{43}$$

$$\begin{aligned}
&\leq \left\| \tilde{\mathbf{1}}(k) \mathbf{1}_n^\top \right\|_2 \left\| \nabla \mathbf{f}(X(k)) - \nabla \mathbf{f}(\mathbf{1}_n (\mathbf{x}^*)^\top) \right\|_F \\
&\leq n\beta \sqrt{b+1} \|X(k) - \mathbf{1}_n (\mathbf{x}^*)^\top\|_F \\
&= n\beta \sqrt{b+1} \left\| \begin{bmatrix} I_n & \mathbf{0} \\ \mathbf{0} & \mathbf{0} \end{bmatrix} \tilde{X}(k) - \begin{bmatrix} \mathbf{1}_n \\ \mathbf{0} \end{bmatrix} (\mathbf{x}^*)^\top \right\|_F \\
&\leq 2n\beta \sqrt{b} \left(\left\| \begin{bmatrix} I_n & \mathbf{0} \\ \mathbf{0} & \mathbf{0} \end{bmatrix} \tilde{X}(k) - \begin{bmatrix} \mathbf{1}_n \\ \mathbf{0} \end{bmatrix} \pi(k-1)^\top \tilde{X}(k) \right\|_F \right. \\
&\quad \left. + \left\| \begin{bmatrix} \mathbf{1}_n (\pi(k-1)^\top \tilde{X}(k) - (\mathbf{x}^*)^\top) \\ \mathbf{0} \end{bmatrix} \right\|_F \right) \\
&\leq 2n\beta \sqrt{b} \left(\left\| \begin{bmatrix} I_n & \mathbf{0} \\ \mathbf{0} & \mathbf{0} \end{bmatrix} - \begin{bmatrix} \mathbf{1}_n \\ \mathbf{0} \end{bmatrix} \pi(k-1)^\top \right\|_F \|\tilde{X}(k)\|_F \right. \\
&\quad \left. + 2n\beta \sqrt{b} \left\| \begin{bmatrix} \mathbf{1}_n (\mathbf{x}_\pi(k) - (\mathbf{x}^*)^\top) \\ \mathbf{0} \end{bmatrix} \right\|_F \right) \\
&\leq 2n\beta \sqrt{b} \left((\sqrt{n} + 1) \|\tilde{X}(k)\|_Q + \sqrt{n} \|\mathbf{x}_\pi(k) - \mathbf{x}^*\|_F \right) \\
&\leq 2n\beta \sqrt{b} \left((\sqrt{n} + 1) \|\tilde{X}(k)\|_Q + \frac{\sqrt{2n}}{\sqrt{\alpha}} \sqrt{f(\mathbf{x}_\pi(k)) - f^*} \right)
\end{aligned}$$

where $\mathbf{x}^* = \text{Proj}_{\mathcal{X}^*}(\mathbf{x}_\pi(k))$ and the last inequality follows from that the Polyak-Łojasiewicz condition implies the quadratic growth condition [40, Theorem 2], i.e., $f(\mathbf{x}) - f^* \geq \frac{\alpha}{2} \|\mathbf{x} - \text{Proj}_{\mathcal{X}^*}(\mathbf{x})\|_2^2, \forall \mathbf{x}$.

Substituting (43) into (42) yields

$$\begin{aligned}
\|\tilde{Y}(k)\|_F &\leq 2n(\sqrt{n} + 1)\beta \sqrt{b} \|\tilde{X}(k)\|_Q + n \|Y_V(k)\|_S \\
&\quad + \frac{2n\beta \sqrt{2nb}}{\sqrt{\alpha}} \tilde{f}(k).
\end{aligned}$$

The desired result is obtained by the definition of $\|\tilde{Y}\|_F^{\lambda, k}$. ■

VII. NUMERICAL EXAMPLES

We use APPG to train a multi-class logistic regression classifier in a distributed manner on the *Covertype* dataset [44], where the objective function takes the following form

$$f(X) = - \sum_{i=1}^{n_s} \sum_{j=1}^{n_c} l_j^i \log \left(\frac{\exp(\mathbf{x}_j^\top \mathbf{s}^i)}{\sum_{j'=1}^{n_c} \exp(\mathbf{x}_{j'}^\top \mathbf{s}^i)} \right) + \frac{\rho}{2} \|X\|_F^2.$$

Here $n_s = 581012$ is the number of training instances, $n_c = 7$ is the number of classes, $n_f = 55$ is the number of features, $\mathbf{s}^i \in \mathbb{R}^{55}$ is the feature vector of the i -th instance, $\mathbf{l}^i = [l_1^i, \dots, l_7^i]^\top$ is the label vector of the i -th instance using the one-hot encoding, $X = [\mathbf{x}_1, \dots, \mathbf{x}_7] \in \mathbb{R}^{n_f \times n_c}$ is the parameters to be optimized, $\rho = 20$ is a regularization factor.

Environment: APPG is implemented in Python 3.6 with OpenMPI 1.10 on Ubuntu 14.04. The hardware is a server with 28 Xeon E5-2660 cores. Each core serves as a computing node.

Distributed Data: We first normalize non-categorical features by subtracting the mean and dividing by the standard deviation in the whole dataset. Then, we *sort* the data by digit label, and sequentially partition it into n parts (with different sizes), where each node (core) only has *exclusive* access to one part. Thus, we are dealing with distributed datasets.

Topology: The directed network among nodes is as follows: Each node i sends messages to node $\text{mod}(2^j + i, n)$, where $j \in \mathbb{N} \cap [0, \log_2(n))$ and $\text{mod}(a, b)$ returns the remainder after division of a by b . Thus, each node has $\mathcal{O}(\log(n))$ out-neighbors, which results in a relatively sparse directed networks. We also implement APPG over other networks in Section VII-B. Note that gossip-based asynchronous algorithms generally cannot work over these directed networks.

Stepsize: The stepsize of each algorithm is tuned via a grid search around $0.5/n_s$.

Local Termination Criteria: Node i stops locally if the value of \mathbf{y}_i in last n consecutive iterations are less than $300/n_s$.

A. Convergence performance and linear speedup

We implement APPG over $n = 1, 6, 12, 18, 24$ nodes ($n = 1$ is used as a baseline since APPG reduces to standard centralized gradient descent method). The training loss w.r.t. running time is plotted in Fig. 6(a), which validates the convergence of APPG, and shows that the training time is significantly reduced with the increase of number of nodes.

Fig. 6(b) plots the training loss of a synchronous version of APPG, which is done by adding a barrier after each update (c.f Section III-C). The result shows that its convergence rate is slower than APPG for $n > 1$.

Fig. 6(c) depicts the training loss w.r.t. the number of iterations. We find that the number of iterations required to achieve the same accuracy is close to each other for different number of nodes. The time for a node to finish an iteration is proportional to the size of its local dataset, and hence is roughly inversely proportional to the number of nodes, which suggests that using n nodes may reduce $\mathcal{O}(n)$ times of training time than that of one node.

To further illustrate this property, we study the speedup of APPG defined as $S_n := T_n/T_1$, where T_n is the running time of the APPG with n node(s) when the training loss decays to 0.005. Fig. 7(a) shows that the APPG achieves a roughly linear speedup in convergence rate w.r.t. the number of nodes. One can also find that the synchronous version of APPG has an approximately linear speedup when the number of cores is small, but it decreases fast when the number of cores is relatively large.

Ideally, the speedup would be n when using n nodes. However, the communication among nodes introduces delays and staleness to the algorithm, which degrades the convergence rate. In practice, a higher speedup than Fig. 7(a) can be achieved by using a low-latency network with larger bandwidth.

B. Effect of network topology

The communication topology may largely affect the convergence performance of distributed algorithms, which is empirically studied in this subsection, where we test the APPG under the following directed graphs.

- (a) `log` topology (default): Node i sends messages to node $\text{mod}(2^j + i, n)$, where $j \in \mathbb{N} \cap [0, \log_2(n))$.
- (b) `sqrt` topology: Node i sends messages to node $\text{mod}(j^2 + i + 1, n)$, where $j \in \mathbb{N} \cap [0, \sqrt{n})$.
- (c) `linear` topology: Node i sends messages to node $\text{mod}(5j + i + 1, n)$, where $j \in \mathbb{N} \cap [0, n/5)$.
- (d) `fully` topology: Fully connected graph, a node sends information to all the rest nodes.

The `log` topology has the sparsest edges while the `fully` topology is the densest one.

Fig. 8(a) shows the convergence rate in running time of 24 cores over these topologies, and Fig. 8(b) depicts the speedup. For `log`, `sqrt` or `linear` topologies, the convergence rate is slightly faster if the graph is denser, which is because a denser graph accelerates the information mixing speed. However, there is a sharp reduction in convergence rate when the graph is too dense as in the `fully` topology. The reason is such a dense graph results in large amount of transmitted data per iteration, which heavily increases the communication overhead and the staleness in gradient computation. In practice, an appropriate topology should be designed according to the network bandwidth and latency.

C. Robustness of APPG to slow cores

We evaluate the robustness of APPG by forcing one core in the network to slow down. This is achieved by adding an artificial waiting time (20ms, a normal iteration takes about 15ms with 24 cores) after each local iteration of a node, which simulates either the slow computation or slow communication.

Fig. 7(b) shows the speedup of the APPG and the synchronous implementation of APPG in this scenario. It indicates that the synchronous counterpart of APPG has a sharp reduction in convergence rate even when only 1 core slows down. In contrast, APPG still keeps an almost linear speedup. This result is also consistent with that in [4], [13].

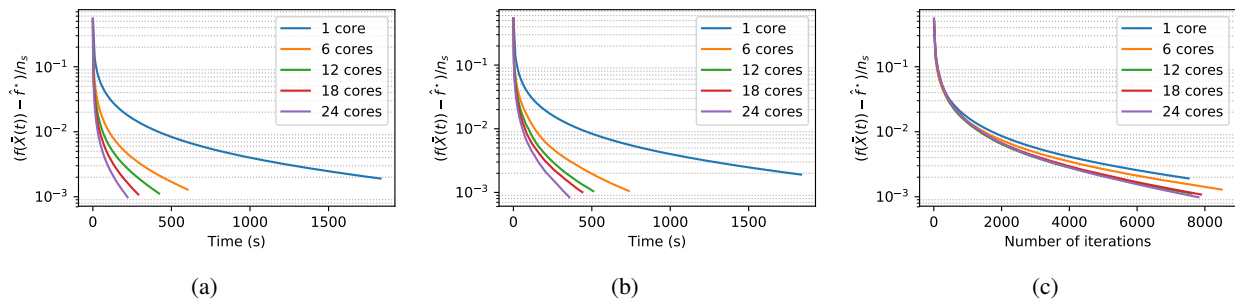


Fig. 6: Convergence performance with different number of nodes. (a) Training loss w.r.t. running time of APPG. (b) Training loss w.r.t. running time of the synchronous version of APPG. (c) Training loss w.r.t. number of iterations (epochs) of APPG.

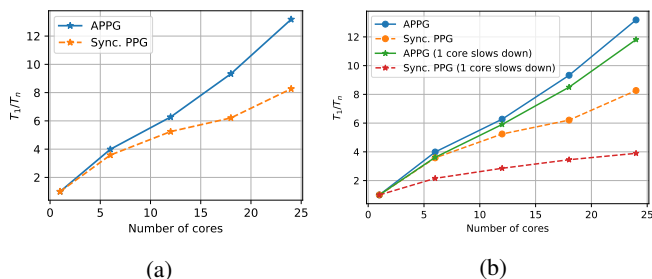


Fig. 7: (a) Speedup in running time of APPG and the synchronous implementation of APPG w.r.t. the number of cores. T_n is the running time of the APPG with n core(s) when the training loss decays to 0.005. (b) Speedup of APPG and the ‘synchronized’ APPG when one core slows down.

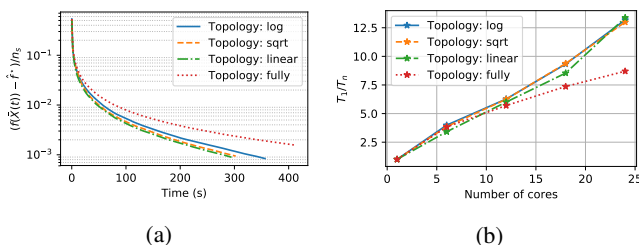


Fig. 8: (a) Convergence rate of APPG using 24 cores over different topologies. (b) Speedup in running time w.r.t. the number of cores over different topologies.

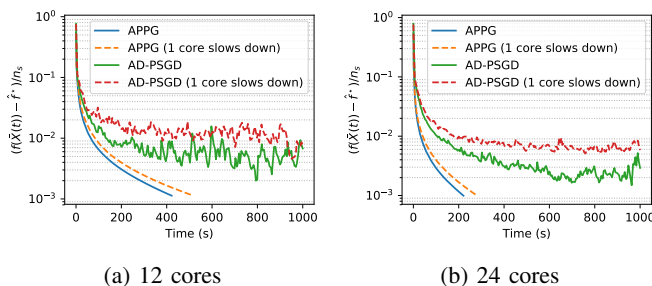


Fig. 9: Convergence of APPG and AD-PSGD with full local gradient when one node is artificially slowed down by adding 20ms waiting time after each iteration.

Introducing the slowing core also brings an easily overlooked problem of asynchronous algorithms, that is, the cores have *uneven* update rates. To show its effect to the performance, we compare the proposed algorithm to a gossip-based asynchronous algorithm AD-PSGD [4] with full local gradients. Note that APPG can only work over *undirected* networks, and hence we modify the network for it by adding a reversed edge to each edge in the directed network, while APPG is still implemented over the directed network. Fig. 9 shows the result over 12 nodes and 24 nodes, where the AD-PSGD fails to converge to the exact optimum. In contrast, APPG converges exactly despite that the convergence rate is reduced a bit.

VIII. CONCLUSION

This paper has proposed a fully asynchronous algorithm (APPG) for distributed optimization. It allows nodes to connect via a directed communication network and update with uncoordinated computation and stale information from neighbors. Linear convergence rate of APPG is achieved for possibly non-convex Lipschitz-smooth functions satisfying the PL condition. The performance of APPG is also demonstrated via a logistic regression problem. Future works may focus on accelerating APPG and extending it to stochastic optimization settings.

REFERENCES

- [1] A. Nedić and N. Ozdaglar, “Distributed subgradient methods for multi-agent optimization,” *IEEE Transactions on Automatic Control*, vol. 54, no. 1, pp. 48–61, 2009.
- [2] P. Lin, W. Ren, and Y. Song, “Distributed multi-agent optimization subject to nonidentical constraints and communication delays,” *Automatica*, vol. 65, pp. 120–131, 2016.
- [3] J. Zhang, K. You, and T. Başar, “Distributed discrete-time optimization in multiagent networks using only sign of relative state,” *IEEE Transactions on Automatic Control*, vol. 64, no. 6, pp. 2352–2367, 2018.
- [4] X. Lian, W. Zhang, C. Zhang, and J. Liu, “Asynchronous decentralized parallel stochastic gradient descent,” in *Proceedings of the 35th International Conference on Machine Learning*, 2018, pp. 3049–3058.
- [5] M. Assran, N. Loizou, N. Ballas, and M. Rabbat, “Stochastic gradient push for distributed deep learning,” in *Proceedings of the 36th International Conference on Machine Learning*, vol. 97, 2019, pp. 344–353.
- [6] J. Zhang and K. You, “Decentralized stochastic gradient tracking for non-convex empirical risk minimization,” *arXiv preprint arXiv:1909.02712*, 2019.
- [7] H. Tang, X. Lian, M. Yan, C. Zhang, and J. Liu, “ D^2 : Decentralized training over decentralized data,” in *Proceedings of the 35th International Conference on Machine Learning*, 2018, pp. 4848–4856.

- [8] T. Wu, K. Yuan, Q. Ling, W. Yin, and A. H. Sayed, "Decentralized consensus optimization with asynchrony and delays," *IEEE Transactions on Signal and Information Processing over Networks*, vol. 4, no. 2, pp. 293–307, 2018.
- [9] A. Nedić, "Asynchronous broadcast-based convex optimization over a network," *IEEE Transactions on Automatic Control*, vol. 56, no. 6, pp. 1337–1351, 2010.
- [10] P. Bianchi, W. Hachem, and F. Iutzeler, "A coordinate descent primal-dual algorithm and application to distributed asynchronous optimization," *IEEE Transactions on Automatic Control*, vol. 61, no. 10, pp. 2947–2957, 2015.
- [11] I. Notarnicola and G. Notarstefano, "Asynchronous distributed optimization via randomized dual proximal gradient," *IEEE Transactions on Automatic Control*, vol. 62, no. 5, pp. 2095–2106, 2016.
- [12] J. Xu, S. Zhu, Y. C. Soh, and L. Xie, "Convergence of asynchronous distributed gradient methods over stochastic networks," *IEEE Transactions on Automatic Control*, vol. 63, no. 2, pp. 434–448, 2018.
- [13] J. Zhang and K. You, "Asyspa: An exact asynchronous algorithm for convex optimization over digraphs," *IEEE Transactions on Automatic Control*, vol. 65, no. 6, pp. 2494–2509, 2020.
- [14] M. Assran, A. Aytekin, H. R. Feyzmahdavian, M. Johansson, and M. G. Rabbat, "Advances in asynchronous parallel and distributed optimization," *Proceedings of the IEEE*, vol. 108, no. 11, pp. 2013–2031, 2020.
- [15] K. I. Tsianos, S. Lawlor, and M. G. Rabbat, "Consensus-based distributed optimization: Practical issues and applications in large-scale machine learning," in *50th Annual Allerton Conference on Communication, Control, and Computing*. IEEE, 2012, pp. 1543–1550.
- [16] Y. Tian, Y. Sun, and G. Scutari, "Achieving linear convergence in distributed asynchronous multi-agent optimization," *IEEE Transactions on Automatic Control*, 2020.
- [17] M. Assran and M. Rabbat, "Asynchronous gradient-push," *IEEE Transactions on Automatic Control*, 2020.
- [18] W. Shi, Q. Ling, G. Wu, and W. Yin, "Extra: An exact first-order algorithm for decentralized consensus optimization," *SIAM Journal on Optimization*, vol. 25, no. 2, pp. 944–966, 2015.
- [19] A. Nedić, A. Olshevsky, and W. Shi, "Achieving geometric convergence for distributed optimization over time-varying graphs," *SIAM Journal on Optimization*, vol. 27, no. 4, pp. 2597–2633, 2017.
- [20] G. Qu and N. Li, "Harnessing smoothness to accelerate distributed optimization," *IEEE Transactions on Control of Network Systems*, 2017.
- [21] K. Scaman, F. Bach, S. Bubeck, Y. T. Lee, and L. Massoulié, "Optimal algorithms for smooth and strongly convex distributed optimization in networks," in *International Conference on Machine Learning*, 2017, pp. 3027–3036.
- [22] Z. Li, W. Shi, and M. Yan, "A decentralized proximal-gradient method with network independent step-sizes and separated convergence rates," *IEEE Transactions on Signal Processing*, vol. 67, no. 17, pp. 4494–4506, 2019.
- [23] J. Xu, Y. Tian, Y. Sun, and G. Scutari, "Distributed algorithms for composite optimization: Unified and tight convergence analysis," *arXiv preprint arXiv:2002.11534*, 2020.
- [24] K. Yuan, B. Ying, X. Zhao, and A. H. Sayed, "Exact diffusion for distributed optimization and learning—part i: Algorithm development," *IEEE Transactions on Signal Processing*, vol. 67, no. 3, pp. 708–723, 2019.
- [25] H. Sun and M. Hong, "Distributed non-convex first-order optimization and information processing: Lower complexity bounds and rate optimal algorithms," *IEEE Transactions on Signal processing*, vol. 67, no. 22, pp. 5912–5928, 2019.
- [26] K. Scaman, F. Bach, S. Bubeck, L. Massoulié, and Y. T. Lee, "Optimal algorithms for non-smooth distributed optimization in networks," in *Advances in Neural Information Processing Systems*, 2018, pp. 2745–2754.
- [27] R. Xin, S. Kar, and U. A. Khan, "Decentralized stochastic optimization and machine learning: A unified variance-reduction framework for robust performance and fast convergence," *IEEE Signal Processing Magazine*, vol. 37, no. 3, pp. 102–113, 2020.
- [28] Y. Lu and C. De Sa, "Moniqua: Modulo quantized communication in decentralized SGD," in *Proceedings of the 37th International Conference on Machine Learning*, ser. Proceedings of Machine Learning Research, vol. 119. Virtual: PMLR, 2020, pp. 6415–6425.
- [29] C. Xi, V. S. Mai, R. Xin, E. H. Abed, and U. A. Khan, "Linear convergence in optimization over directed graphs with row-stochastic matrices," *IEEE Transactions on Automatic Control*, vol. 63, no. 10, pp. 3558–3565, 2018.
- [30] P. Xie, K. You, R. Tempo, S. Song, and C. Wu, "Distributed convex optimization with inequality constraints over time-varying unbalanced digraphs," *IEEE Transactions on Automatic Control*, vol. 63, no. 12, pp. 4331–4337, 2018.
- [31] A. Nedić and A. Olshevsky, "Distributed optimization over time-varying directed graphs," *IEEE Transactions on Automatic Control*, vol. 60, no. 3, pp. 601–615, 2015.
- [32] G. Scutari and Y. Sun, "Distributed nonconvex constrained optimization over time-varying digraphs," *Mathematical Programming*, vol. 176, no. 1–2, pp. 497–544, 2019.
- [33] S. Pu, W. Shi, J. Xu, and A. Nedic, "Push-pull gradient methods for distributed optimization in networks," *IEEE Transactions on Automatic Control*, pp. 1–1, 2020.
- [34] R. Xin and U. A. Khan, "A linear algorithm for optimization over directed graphs with geometric convergence," *IEEE Control Systems Letters*, vol. 2, no. 3, pp. 315–320, July 2018.
- [35] F. Saadatniaiki, R. Xin, and U. A. Khan, "Decentralized optimization over time-varying directed graphs with row and column-stochastic matrices," *IEEE Transactions on Automatic Control*, vol. 65, no. 11, pp. 4769–4780, 2020.
- [36] J. Tsitsiklis, D. Bertsekas, and M. Athans, "Distributed asynchronous deterministic and stochastic gradient optimization algorithms," *IEEE Transactions on Automatic Control*, vol. 31, no. 9, pp. 803–812, 1986.
- [37] S. Li and T. Başar, "Asymptotic agreement and convergence of asynchronous stochastic algorithms," *IEEE Transactions on Automatic Control*, vol. 32, no. 7, pp. 612–618, 1987.
- [38] A. Spiridonoff, A. Olshevsky, and I. C. Paschalidis, "Robust asynchronous stochastic gradient-push: Asymptotically optimal and network-independent performance for strongly convex functions," *Journal of Machine Learning Research*, vol. 21, no. 58, pp. 1–47, 2020.
- [39] M. Fazel, R. Ge, S. Kakade, and M. Mesbahi, "Global convergence of policy gradient methods for the linear quadratic regulator," in *Proceedings of the 35th International Conference on Machine Learning*, vol. 80, 2018, pp. 1467–1476.
- [40] H. Karimi, J. Nutini, and M. Schmidt, "Linear convergence of gradient and proximal-gradient methods under the Polyak-Lojasiewicz condition," in *Joint European Conference on Machine Learning and Knowledge Discovery in Databases*. Springer, 2016, pp. 795–811.
- [41] A. Nedić and A. Ozdaglar, "Convergence rate for consensus with delays," *Journal of Global Optimization*, vol. 47, no. 3, pp. 437–456, 2010.
- [42] B. Touri, *Product of random stochastic matrices and distributed averaging*. Springer Science & Business Media, 2012.
- [43] A. Nedić and A. Olshevsky, "Stochastic gradient-push for strongly convex functions on time-varying directed graphs," *IEEE Transactions on Automatic Control*, vol. 61, no. 12, pp. 3936–3947, 2016.
- [44] D. Dheeru and E. Karra Taniskidou, "UCI machine learning repository," 2017. [Online]. Available: <http://archive.ics.uci.edu/ml>